THE JOURNAL OF PHYSICAL CHEMISTRY A

Article

pubs.acs.org/JPCA

Revisiting the Kinetics and Thermodynamics of the Low-Temperature Oxidation Pathways of Alkanes: A Case Study of the Three Pentane Isomers

John Bugler, Kieran P. Somers, Emma J. Silke, and Henry J. Curran*

Combustion Chemistry Centre, National University of Ireland, Galway, Ireland

ABSTRACT: This paper describes our developing understanding of low-temperature oxidation kinetics. We have investigated the ignition of the three pentane isomers in a rapid compression machine over a wide range of temperatures and pressures, including conditions of negative temperature coefficient behavior. The pentane isomers are small alkanes, yet have structures that are complex enough to allow for the application of their kinetic and thermochemical rules to larger molecules. Updates to the thermochemistry of the species important in the low-temperature oxidation of hydrocarbons have been made based on a thorough literature review. An evaluation of recent quantum-chemically derived rate coefficients from the literature pertinent to important low-temperature oxidation reaction classes has been performed, and new rate rules are recommended for these classes. Several reaction classes have also been included to determine their importance with regard to simulation results, and we have found that they should be included when developing future chemical kinetic mechanisms. A comparison of the model simulations with pressure-time histories from experiments in a rapid compression machine shows very good agreement for both ignition delay time and pressure rise for both the first- and second-stage ignition events. We show that revisions to both the thermochemistry and the kinetics are required in order to replicate experiments well. A broader validation of the models with ignition delay times from shock tubes and a rapid compression machine is presented in an accompanying paper. The results of this study enhance our understanding of the combustion of straight- and branched-chained alkanes.

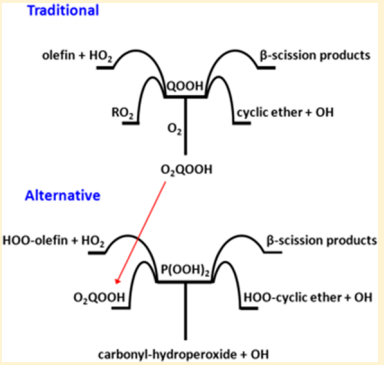

1. INTRODUCTION

Alkanes are the simplest type of hydrocarbon, so knowledge of the combustion of these compounds is essential to the fundamental understanding of the combustion of all hydrocarbons and oxygenated fuels (e.g., alcohols, large methyl esters, etc.). The low-temperature oxidation of alkanes is of practical importance to the advancement of technologies such as homogeneous-charge compression-ignition (HCCI), premixed-charge compression-ignition (PCCI), and reactivity-controlled compression-ignition (RCCI) engines. Construction of detailed mechanisms describing low-temperature oxidation can be difficult due to the large number of chemical species and reactions involved. Group additivity[1] and rate rule[2,3] methods are convenient solutions to this problem. In this study, we discuss the implementation of both methods, and improved values used therein, for current and future development of detailed chemical kinetic models.

The first low-temperature reaction channels for the oxidation of alkanes were proposed in the late 1960s by Knox[4] and Fish.[5] An improved understanding was developed by Pollard,[6] Cox and Cole,[7] and Walker and Morley.[8] Curran et al. applied rate coefficients based on rate estimation rules for different reaction classes and had success in modeling the oxidation of *n*-heptane and *iso*-octane at low temperatures.[2,3] However, some reaction classes were excluded from the low-temperature reaction pathways of these mechanisms due to limitations in knowledge at the time. These involve hydroperoxyl-alkyl-peroxyl ($\dot{O}_2QOOH$) radicals undergoing reactions similar to those included for alkyl-peroxyl ($R\dot{O}_2$) species, such as the direct elimination of $H\dot{O}_2$ radicals from the alkyl-peroxyl radicals (also forming olefins), and isomerization reactions like those of $R\dot{O}_2$ radicals to produce hydroperoxyl-alkyl ($\dot{Q}OOH$) radicals, but resulting in the formation of dihydroperoxyl-alkyl radicals. These can undergo reactions similar to those of $\dot{Q}OOH$ radicals, such as cyclic ether formation, and β-scission reactions (Figure 1, R, Q, and P represent alkyl radicals or structures C_nH_{2n+1}, C_nH_{2n}, and C_nH_{2n-1}, respectively). Inclusion of these "alternative" reaction classes are of particular importance for the mechanisms of branched alkanes, as previously,[3] the chain of reactions proceeding from tertiary alkyl radical addition to molecular oxygen came to a "dead end" upon formation of an $\dot{O}_2QOOH$ radical, as these radicals cannot produce a carbonyl-hydroperoxide + $\dot{O}H$. An example of this for *iso*-pentane is shown in Figure 2. This means that any $\dot{O}_2QOOH$ species formed from successive pathways stemming from a tertiary alkyl radical had no mechanism to decompose other than

Special Issue: 100 Years of Combustion Kinetics at Argonne: A Festschrift for Lawrence B. Harding, Joe V. Michael, and Albert F. Wagner

Received: January 27, 2015
Revised: March 18, 2015
Published: March 23, 2015

DOI: 10.1021/acs.jpca.5b00837
J. Phys. Chem. A 2015, 119, 7510−7527

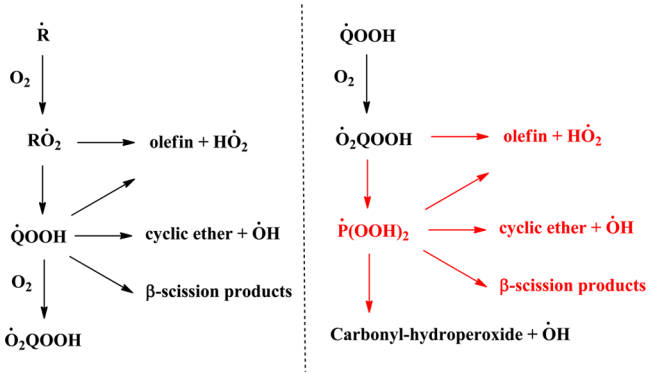

Figure 1. Lumped kinetic scheme of the primary oxidation reactions of alkanes. Species and arrows highlighted in red represent pathways not previously considered for the pentane isomers.

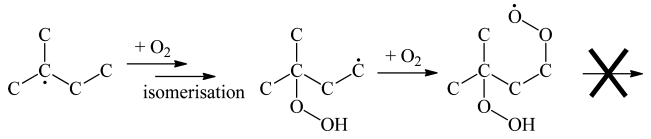

Figure 2. Example of a "dead end" in low-temperature pathways of *iso*-pentane. The example $\dot{O}_2QOOH$ shown cannot form a carbonyl-hydroperoxide + ȮH.

dissociation back to $\dot{Q}OOH + O_2$. This represents quite a mechanistic oversight in the modeling of branched alkanes.

Silke[9] and Glaude et al.[10] have performed studies of some of these alternative reaction classes for the low-temperature oxidation of *n*-heptane. A simplified scheme for the primary oxidation reactions of alkanes, including these "alternative" reaction classes is shown in Figure 1. Silke[9] added the following reaction classes to the *n*-heptane mechanism published by Curran et al.:[2] $\dot{O}_2QOOH \rightleftharpoons \dot{P}(OOH)_2$; $\dot{P}(OOH)_2 \leftrightarrow$ cyclic ether + ȮH; $R\dot{O}_2 + \dot{O}H \leftrightarrow R\dot{O} + H\dot{O}_2$; $R\dot{O}_2 + H\dot{O}_2 \leftrightarrow ROOH + O_2$; $\dot{Q}OOH$ intramolecular isomerization; and $R\dot{O}_2 \leftrightarrow$ olefin + $H\dot{O}_2$.

Silke found that, of the classes added, those that had the largest effect on simulated ignition delay times (IDTs) were $\dot{O}_2QOOH \rightleftharpoons \dot{P}(OOH)_2$ and $\dot{P}(OOH)_2 \leftrightarrow$ cyclic ether + ȮH. Examples of these types of reactions for *n*-pentane are shown in Figure 3.

Silke[9] assigned rate coefficients to the new reaction classes by making analogies to similar reactions (i.e., rate coefficients for $\dot{O}_2QOOH \rightleftharpoons \dot{P}(OOH)_2$ isomerization reactions were based on those for $R\dot{O}_2 \rightleftharpoons \dot{Q}OOH$). For the reactions $\dot{P}(OOH)_2 \leftrightarrow$ cyclic ether + ȮH, the rate coefficients used for $\dot{Q}OOH \leftrightarrow$ cyclic ether + ȮH were adopted. The rate coefficients used were those recommended by Curran et al.[2,3] Inclusion of these classes led to large changes in simulated IDTs, to the extent that the model no longer predicted the experimental measurements (Figure 4). The attempted improvement of the *n*-heptane mechanism did not result in better agreement with experiments. Thus, the rate rules used were not compatible with the consideration of these alternative reactions. However, it is essential that these pathways are included to ensure a detailed understanding of a fuel's oxidation. The fact that the rate rules of Curran et al.[2,3] were not suitable for application to the alternative pathways, yet the predictions of the *n*-heptane[2] and *iso*-octane[3] models reproduced data very well, points to a lack of fundamental understanding of the thermochemical

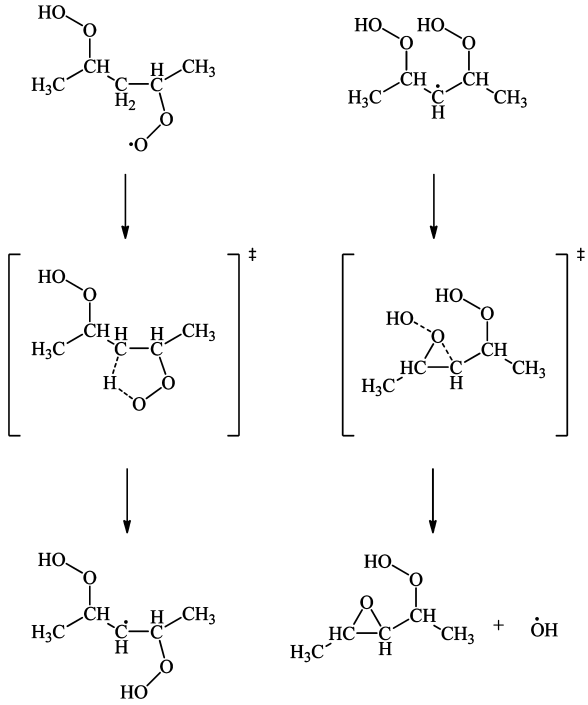

Figure 3. Examples of reaction classes applied to *n*-pentane in this work, which were previously added to Silke[9] *n*-heptane mechanism (a) "alternative" isomerization of $\dot{O}_2QOOH$. (b) Hydroperoxyl cyclic ether formation from $\dot{P}(OOH)_2$.

parameters, rate coefficients, and/or both in the previous studies.

In their work on *iso*-octane, Curran et al.[3] reduced the rate coefficients for the isomerization reactions of $R\dot{O}_2$ and $\dot{O}_2QOOH$ radicals by a factor of 3 relative to those employed for *n*-heptane in order to match experimental data at low temperatures (600−770 K). It was postulated that there must be a reason that these reactions were slower for *iso*-octane than for *n*-heptane, or that there must have been pathways missing in the mechanism. With such discrepancies existing for the primary reference fuels (PRFs), it was clear that a re-examination of the thermochemistry and rate coefficients pertaining to the low-temperature oxidation pathways of alkanes was needed in order to reconcile these differences. It is for this reason that the pentane isomers were selected in this study. They are small enough to allow for an in-depth study of their low-temperature oxidation pathways yet large enough to be representative of larger alkanes. The proximity of the outermost secondary carbons in *n*-pentane makes it an ideal analogue for longer *n*-alkanes, due to isomerization reactions of $R\dot{O}_2$ and $\dot{O}_2QOOH$ radicals between these carbons being dominant, controlling pathways at low temperatures. The different levels of structural branching of *iso*- and *neo*-pentane make them suitable analogues for longer branched-chained alkanes, such as *iso*-octane, with both isomers being representative of the varyingly branched ends of the *iso*-octane molecule.

There have been a number of recent systematic studies which have used various computational quantum chemical methods for rate coefficient calculations for reactions relevant to the low-temperature oxidation of alkanes.[12−17] These studies have calculated high-pressure limit rate coefficients for sets of training reactions so that they can be used directly in chemical kinetic mechanisms for combustion relevant applications. To

DOI: 10.1021/acs.jpca.5b00837
J. Phys. Chem. A 2015, 119, 7510−7527

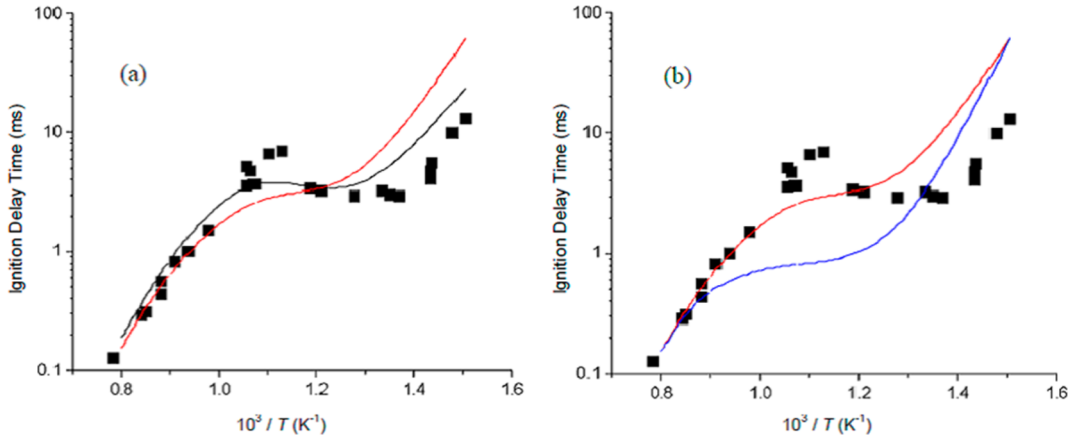

Figure 4. Effect of (a) "alternative" isomerisations of $\dot{O}_2QOOH$ and (b) hydroperoxyl cyclic ether formation from $\dot{P}(OOH)_2$ for *n*-heptane, Φ = 1.0 in "air", ~13.5 atm.[9] (■) Ciezki et al.;[11] (—) Curran et al.;[2] (red —) model including "alternative" isomerisations; (blue —) model including "alternative" isomerisations and hydroperoxyl cyclic ether formation. All simulations shown are at constant volume conditions.

Table 1. Comparison of Original and Updated Group Additivity Values at 298.15 K for Selected Groups

	original		updated	
	enthalpy, $H°$ (kcal mol^{-1})	entropy, $S°$ (cal mol^{-1} K^{-1})	enthalpy, $H°$ (kcal mol^{-1})	entropy, $S°$ (cal mol^{-1} K^{-1})
C/C/H2/OO	−7.89	9.65	−8.02	6.62
C/C2/H/OO	−6.08	−11.96	−7.03	−15.46
OO/C/H	−23.50	36.84	−20.60	38.64
ALPEROX	86.30	0.22	85.27	−0.48

our knowledge, these rate coefficients have not been applied to all of the important reaction classes in the low-temperature regime in a hydrocarbon oxidation mechanism. In this work, the rate coefficients from these studies are compared and have been applied to the mechanisms of the pentane isomers. The model simulations are compared to sample ignition delay times in addition to pressure−time histories obtained in a rapid compression machine (RCM). A detailed description of the RCM design can be found in ref 18. On the basis of these theoretical studies, new recommended rate rules are proposed and are also tested in mechanisms to evaluate their performance against ignition delay times.

A more thorough validation of the mechanisms across a broader range of temperatures, pressures, and with data from other experimental facilities, along with a description of the facility used to obtain the data presented herein, will be discussed in an accompanying paper.[19] This study provides a systematic evaluation of the rate rules in the literature and their suitability for application to mechanisms for the low-temperature oxidation of straight-chained, branched-chained, and highly branched alkanes and will propose new rate rule recommendations for application to larger alkanes. This will be particularly important for the construction of gasoline surrogate mechanisms.

2. MODEL DEVELOPMENT

Healy et al.[20] previously developed a mechanism to describe *n*-pentane oxidation based on rate rules recommended by Curran et al.[2,3] This mechanism did not include any of the alternative reaction classes but has served as a starting point for the current investigation.

2.1. Thermochemistry. Previously,[2,3,9,20,21] the thermochemical data for species were estimated using group additivity rules derived by Benson[1] and implemented in THERM.[22] Due to improved computational methods for calculation of thermochemical properties and a growing amount of literature data, a thorough literature review of thermochemical properties was undertaken for C_1−C_4 alkanes, alkenes, alcohols, hydroperoxides, alcoholic hydroperoxides, and their associated radicals.[23] A variety of sources, including high-level ab initio studies, experimental studies, online databases, and review studies has led to updated group additivity values which have been used to update the thermochemistry of the following classes of C_5 species: fuel (RH), fuel radicals ($\dot{R}$), olefins, alkyl hydroperoxides (RO_2H), alkyl-peroxyl radicals ($R\dot{O}_2$), hydroperoxyl alkyl radicals ($\dot{Q}OOH$), cyclic ethers, hydroperoxyl-alkyl-peroxyl radicals ($\dot{O}_2QOOH$), and carbonyl-hydroperoxides, as well as any species produced through pathways which have been added to the mechanisms, which will be discussed in detail later.

The most significant changes are to the values of the groups listed in Table 1. C/C/H2/OO refers to the carbon at the terminus of an alkyl chain and α- to a hydroperoxyl group (R−CH_2OOH). C/C2/H/OO represents an internal carbon in an alkyl chain, bonded to two other carbons and a hydroperoxyl group (R−CH(OOH)−R′). OO/C/H represents a hydroperoxyl group bonded to a carbon atom (R−C(OOH)(R′)−R″), and ALPEROX refers to a peroxyl radical (R−O$\dot{O}$).

The C/C/H2/OO and C/C2/H/OO groups were optimized based on the newly recommended values for ethyl, *n*-propyl, *iso*-propyl, *n*-butyl, and *s*-butyl hydroperoxides, and their associated peroxyl radicals. The enthalpies increased from those previously used, and the entropies decreased for all of these species, resulting in the Gibbs energies increasing by approximately 2.1−3.4 kcal mol^{-1} at 298.15 K when the new group values are applied. The OO/C/H group was also optimized based on the aforementioned alkyl hydroperoxide and alkyl-peroxyl radical species but also included hydroperoxyl-ethanol and hydroperoxyl-*n*-propanol and their asso-

DOI: 10.1021/acs.jpca.5b00837
J. Phys. Chem. A 2015, 119, 7510−7527

ciated peroxyl radicals. Both the enthalpies and entropies for the hydroperoxyl alcohols and their associated peroxyl radicals decreased from those which had previously been used. This resulted in the Gibbs energies of these species varying approximately from −0.6 to +0.5 kcal mol^{-1} at 298.15 K. The optimization of the ALPEROX group was based on the updated values of the aforementioned alkyl-peroxyl radicals, the enthalpy and entropy values of which (as mentioned previously) increased and decreased, respectively, resulting in an increase in Gibbs energy values of approximately 2.1−2.5 kcal mol^{-1} at 298.15 K.

Figure 5 illustrates the changes in values of thermochemical properties for species important in the low-temperature

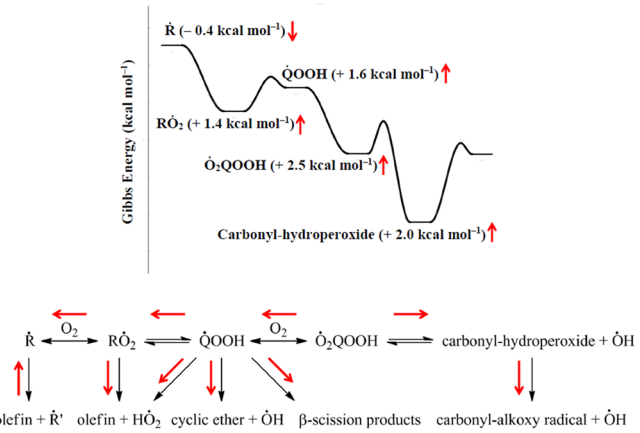

Figure 5. Representation of average changes in Gibbs energies at 298.15 K for important classes of species due to updated THERM group values for *n*-pentane and subsequent shifts in equilibria for important reaction classes.

combustion regime for *n*-pentane, as well as the shifts in equilibria for the main reaction pathways they participate in, brought about by the changes in the thermochemical values.

The inclusion of the updated thermochemistry led to a significant decrease in reactivity (Figure 6) due to changes in

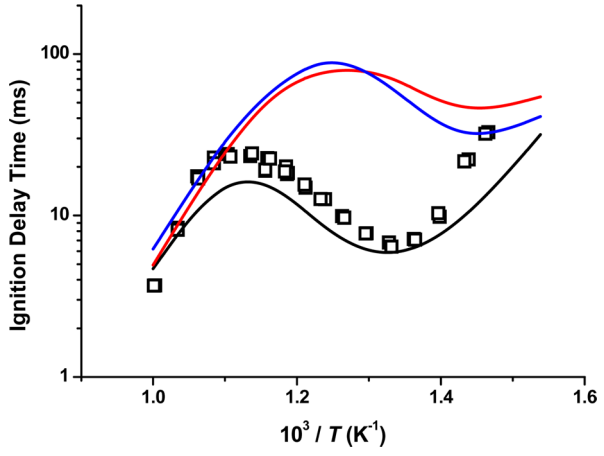

Figure 6. Effect of updated thermochemistry and submechanism. *n*-Pentane, Φ = 1.0 in "air", 10 atm. Symbols represent IDTs from an RCM. (—) Model predictions using original thermochemistry; (red —) model predictions using updated thermochemistry; (blue —) model predictions using updated thermochemistry and C_0−C_4 submechanism.[24−27] All simulations shown are at constant volume conditions.

the equilibria of the reactions involving the updated species (Figure 5). The main shifts in equilibria are for the reactions of RȮ$_2$, Q̇OOH, and Ȯ$_2$QOOH radicals, with dissociation of RȮ$_2$ and Ȯ$_2$QOOH radicals back to their respective alkyl and hydroperoxyl-alkyl radicals and molecular oxygen becoming more dominant, as well as the chain propagating reactions of RȮ$_2$ and Q̇OOH radicals (which curtail progression toward chain branching reactions) also becoming more dominant. With the updated thermochemistry, there is more flux from Ȯ$_2$QOOH radicals to produce carbonyl-hydroperoxides + ȮH, and subsequently the decomposition of carbonyl-hydroperoxides to yield a second hydroxyl radical and a carbonyl-alkoxyl radical. These steps constitute chain branching as three radicals are formed from the initial Ȯ$_2$QOOH species, but the effect of the shifts in equilibria on reactivity is minimal due to the large changes in flux earlier in the chain of reactions, involving Ṙ, RȮ$_2$, and Q̇OOH radicals, leading to their formation. These results show that, with the adjusted thermochemistry of species relevant to the low-temperature combustion of *n*-pentane, updates to the rate coefficients important to low-temperature oxidation were necessary. This began with an update to the C_0−C_4 submechanism,[24−27] with the results showing a relatively minor influence when compared to that of the updated thermochemistry (Figure 6). It is clear that major changes were needed in the rate coefficients used for the C_5 reactions. These updates will form the basis of our later discussion.

2.2. Chemical Kinetic Mechanism. Villano et al.[12,13] systematically calculated high-pressure limit rate coefficients for the low-temperature oxidation reactions of alkanes, including the pentane isomers, using the CBS-QB3 quantum chemical method combined with canonical transition state theory calculations. Karwat et al.[28] studied the oxidation of *n*-heptane in a rapid compression facility and demonstrated success in applying the Villano et al. rate rules. However, Villano et al.[12,13] did not calculate rate coefficients for the alternative reaction classes that were investigated in this work, and so rate coefficients for these reactions are based by analogy with similar reactions. Rate coefficients for each reaction in the following reaction classes have been applied directly from the studies of Villano et al.:[12,] concerted elimination of HȮ$_2$ from alkyl-peroxyl radical (RȮ$_2$ ↔ olefin + HȮ$_2$); *β*-scission of hydroperoxyl-alkyl radical to produce an olefin + HȮ$_2$ (Q̇OOH ↔ olefin + HȮ$_2$); cyclic ether formation from hydroperoxyl-alkyl radical (Q̇OOH ↔ cyclic ether + ȮH); and *β*-scission of hydroperoxyl-alkyl radical to produce other products (Q̇OOH ↔ *β*-scission products).

2.2.1. Ṙ + O_2 and Q̇OOH + O_2 Addition Reactions. Miyoshi used variational transition state theory (VTST) and Rice-Ramsperger-Kassel-Marcus theory (RRKM)/master equation calculations based on the CASPT2(7,5)/aug-cc-pVDZ//B3LYP/6-311G(d,p) potential energy curves and B3LYP/6-311G(d,p) geometries and vibrational frequencies, for archetypal alkyl radical (Ċ$_2$H$_5$, *i*-Ċ$_3$H$_7$, *n*-Ċ$_4$H$_9$, *s*-Ċ$_4$H$_9$, and *t*-Ċ$_4$H$_9$) + O$_2$ reactions, and obtained class-specific high-pressure limit rate coefficients for these systems.[14] Rate coefficients for the addition of Ṙ to O$_2$, and Q̇OOH to O$_2$, have been calculated by Goldsmith et al. for the propyl + O$_2$ system, using variable reaction coordinate transition state theory (VRC-TST) calculations.[15] The rate coefficients calculated by Goldsmith et al. for additions to primary and secondary alkyl radical sites are approximately factors of two and five times faster, respectively, than those calculated by Miyoshi. We find that

DOI: 10.1021/acs.jpca.5b00837
J. Phys. Chem. A 2015, 119, 7510−7527

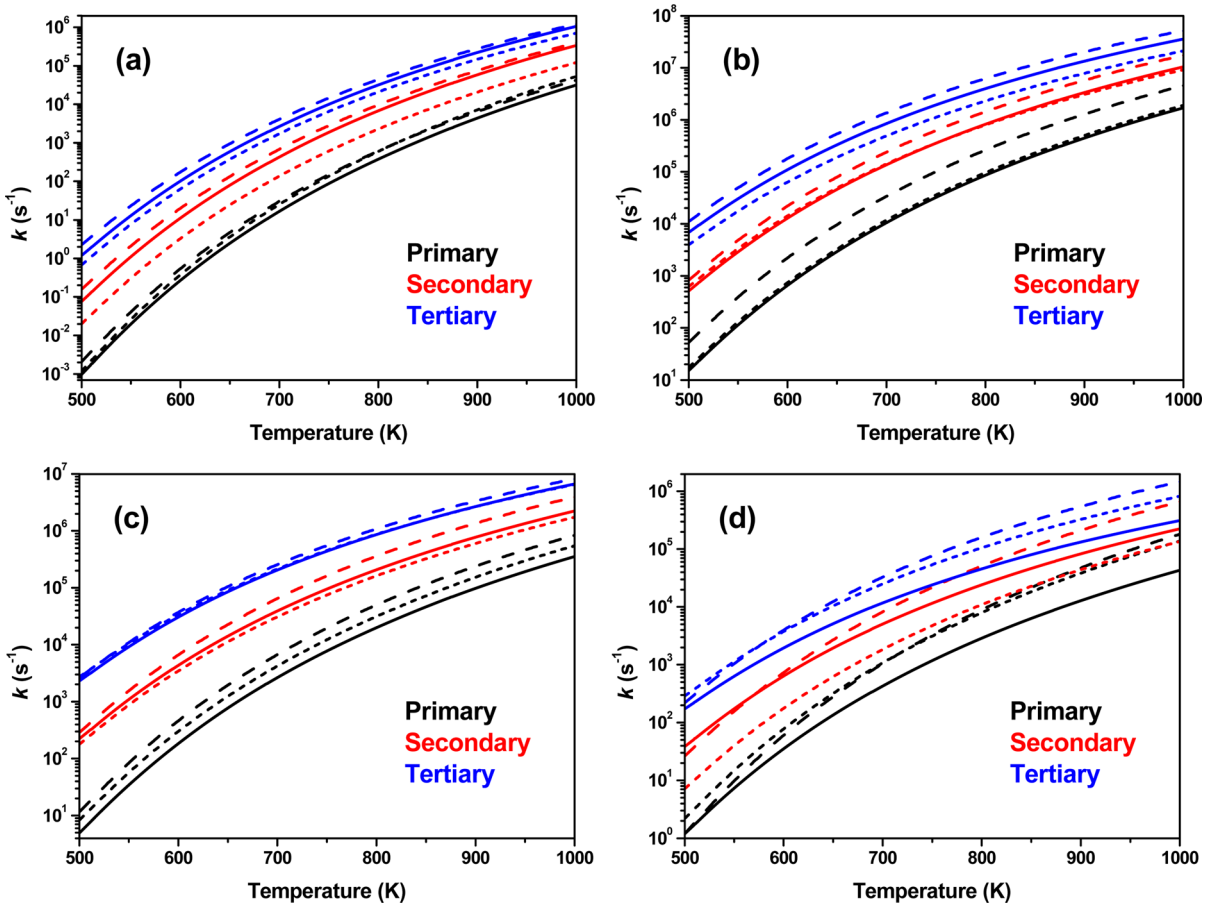

Figure 7. Averaged rate coefficients for reactions of $R\dot{O}_2 \rightleftharpoons \dot{Q}OOH$ progressing through (a) 5-, (b) 6-, (c) 7-, and (d) 8-membered TS rings. Solid lines correspond to Villano et al.,[12] dashed lines correspond to Miyoshi,[16] and dotted lines correspond to Sharma et al.[17]

using the rate coefficients calculated by Goldsmith et al.[15] for both first and second additions results in ignition delay time simulations that are faster than experimental measurements for the pentane isomers. Instead, the rate coefficients for addition of $\dot{R}$ to O_2 are adopted from Miyoshi, and those used for addition of $\dot{Q}OOH$ to O_2 are based on these first addition rate coefficients, with the A-factor scaled based on the results of Goldsmith et al.[15] Their work reported that the $\dot{Q}OOH + O_2$ reaction is typically slower than the analogous $\dot{R} + O_2$ reaction by approximately a factor of 2, with the exception of the addition of $HOOCH_2CH_2\dot{C}H_2$, which is faster than the analogous first addition to O_2. For each of the pentanes, we find that a reduction of the second addition to O_2 by approximately a factor of 2 results in experimental data being well reproduced by model simulation results.

Zádor et al.[29] performed the first experimental measurements of rate coefficients for the $\dot{Q}OOH + O_2$ addition reaction. They determined the rate coefficient for the association reaction of 2-hydroperoxyl-2-methylprop-1-yl with O_2 to be $(5.4 \pm 1.8) \times 10^{11}$ cm^3 mol^{-1} s^{-1}. This is supported by VRC-TST calculations performed as part of the same study, and this value is in excellent agreement (within 50% between 600 and 1000 K) with the estimated rate coefficients for the addition of a primary radical site on $\dot{Q}OOH$ radicals to O_2 within the submechanisms of the pentane isomers.

2.2.2. $R\dot{O}_2$ and $\dot{O}_2QOOH$ Isomerization Reactions. Villano et al.,[12] Miyoshi,[16] and Sharma et al.[17] all calculated rate coefficients for $R\dot{O}_2 \rightleftharpoons \dot{Q}OOH$ isomerization reactions for sets of sample reactions using the CBS-QB3 quantum chemical method. Figure 7 shows comparisons of the averaged rate coefficients for this reaction class from these three studies.[12,16,17] All rate coefficients are compared on a per H-atom basis. There is good agreement between the literature values, most being within a factor of 2−3 of one another, with a maximum discrepancy of approximately a factor of 5 for reactions proceeding through an 8-membered transition state (TS) ring at 1000 K. As will be shown in an accompanying paper,[19] when applied to the mechanisms of the pentane isomers the rate coefficients for the H-shift reactions of $R\dot{O}_2 \rightleftharpoons \dot{Q}OOH$ through 6-membered TS rings are the most important, with a relatively high flux proceeding through these pathways.

Figure 8 shows the effect of using the rate coefficients for the first isomerization reactions calculated from each of the three studies on the simulated ignition delay times of each of the pentane isomers, as well as treating the second isomerization reactions as recommended by Curran et al.[2,3] That is, using analogous reactions of $R\dot{O}_2 \rightleftharpoons \dot{Q}OOH$ to estimate the second isomerization reaction, by using the same pre-exponential factors as the reaction being used in the analogy (while at the same time accounting for degeneracy) and reducing the activation energy by 3 kcal mol^{-1}.

It is shown that using the rate coefficients from any of the three aforementioned studies[12,16,17] and treating the second isomerization reactions as recommended by Curran et al.[2,3] results in similar simulated ignition delay times for each of the three isomers. This reflects the general similarity between each

DOI: 10.1021/acs.jpca.5b00837
J. Phys. Chem. A 2015, 119, 7510−7527

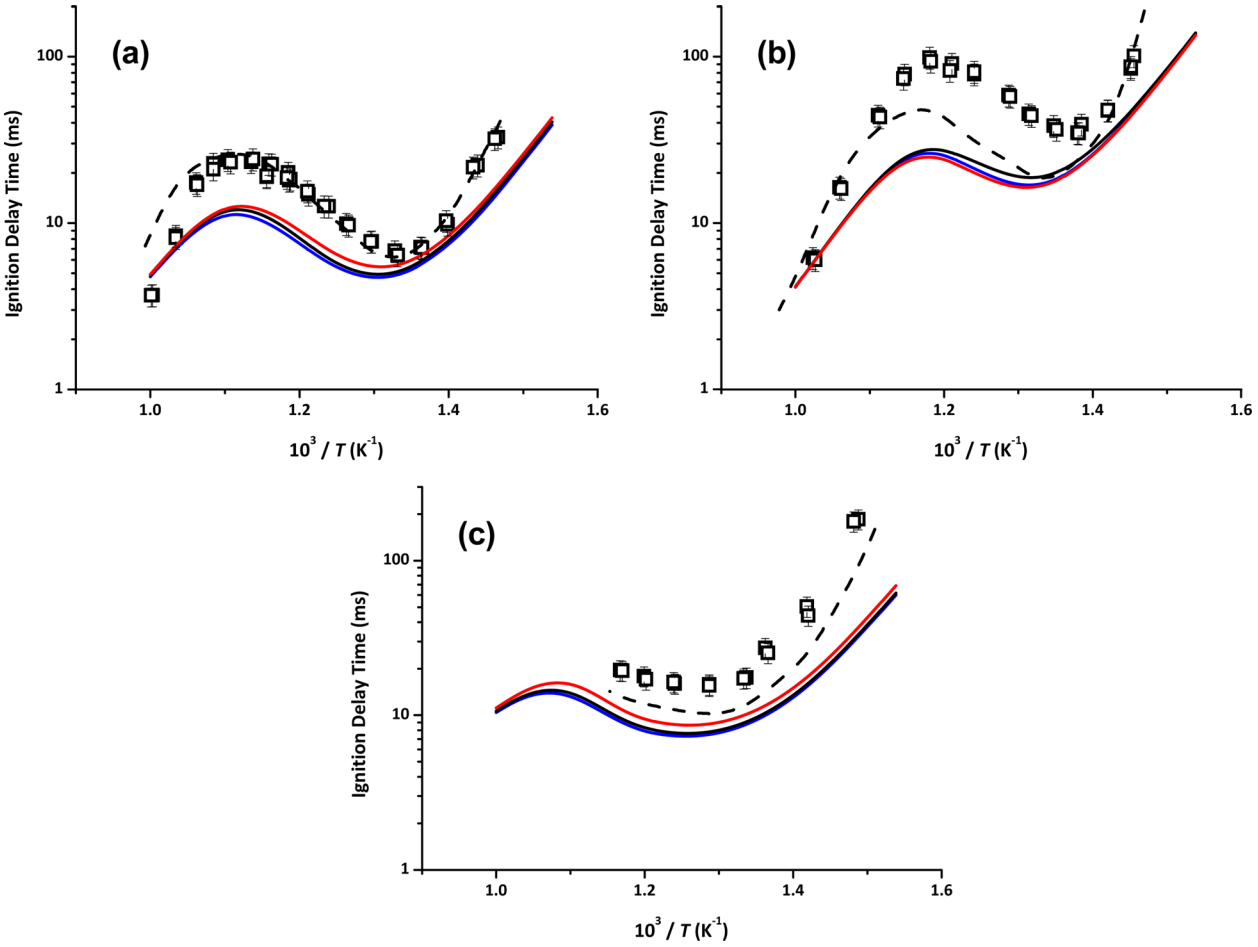

Figure 8. Effect of using calculated rate coefficients for $R\dot{O}_2 \rightleftharpoons \dot{Q}OOH$ of (—) Sharma et al.,[17] (red —) Miyoshi,[16] and (blue —) Villano et al.[12] on IDT simulations as well as treating the second isomerization reactions as recommended by Curran et al.[2,3] for (a) *n*-pentane, (b) *iso*-pentane, and (c) *neo*-pentane. Open symbols represent ignition delay times for (a) *n*-, (b) *iso*-, and (c) *neo*-pentane: all at Φ = 1.0 in "air", 10 atm. Dashed lines correspond to simulations using the rate coefficients of Sharma et al.[17] and accounting for facility effects in the RCM.

of the calculated rate coefficients for the first isomerization reactions, since the second isomerization reactions are treated by analogy to these. While good agreement is observed between simulations and experiments for *n*-pentane, it is not the case for *iso*- or *neo*-pentane, for which the simulated ignition delay times are faster compared to the experiments (Figure 8).

The last important reaction pathway for which calculated rate coefficients have not been added is the isomerization reaction $\dot{O}_2QOOH \rightleftharpoons$ carbonyl-hydroperoxide + $\dot{O}H$. Miyoshi[16] and Sharma et al.[17] have both calculated this class of reactions for sets of training reactions using the CBS-QB3 quantum chemical method. However, Sharma et al. propose an alternative hindered-rotor treatment for $\dot{O}_2QOOH$ radicals, due to these molecules having multiple internal rotors with potentials that are not independent of each other. They find that interactions between the oxygen and hydrogen atoms within the molecule results in a lowest energy conformer that has a ring shape, with the peroxyl group forming a hydrogen bond with the OOH group. Comparisons of the rate coefficients show general trends, Figure 9, where "primary" refers to abstraction by the peroxyl moiety of a hydrogen bonded to the terminal carbon on an alkyl chain, which is in turn adjacent to a hydroperoxyl moiety (e.g., $\dot{O}_2CH_2CH_2CH_2OOH \rightleftharpoons HO_2CH_2CH_2CHO + \dot{O}H$). "Secondary" refers to the same type of reaction but with the abstracted hydrogen instead bonded to an internal carbon (e.g., $\dot{O}_2CH_2CH(OOH)CH_3 \rightleftharpoons HO_2CH_2C{=}OCH_3 + \dot{O}H$). Rate coefficients calculated by Sharma et al. for reactions which proceed through 5-membered TS rings are, in general, faster than those calculated by Miyoshi (although those proceeding through the "primary" pathways are roughly equal), whereas reactions proceeding through 6-, 7-, and 8-membered rings are generally slower.

Figure 10 shows the effects of using the rate coefficients calculated by Miyoshi and by Sharma et al. for the isomerization reactions of $\dot{O}_2QOOH$ (specifically, the ones which involve abstraction of a hydrogen atom from the carbon attached to the OOH group, producing a carbonyl-hydroperoxide + $\dot{O}H$) on simulated ignition delay times. Comparing Figures 8 and 10, we see that for each of the pentane isomers, using Miyoshi's rate coefficients for both the first and second isomerization reactions, yields similar results to using Miyoshi's first isomerization rate coefficients and treating the second isomerization reactions by analogy to these (i.e., by using the same pre-exponential factors as the reaction being used in the analogy, while at the same time accounting for degeneracy, and reducing the activation energy by 3 kcal mol^{-1}). While similar results are seen when applying the rate coefficients of Miyoshi[16] and Sharma et al.[17] to the first and second isomerization reactions of *n*- and *neo*-pentane (Figure 10, panels a and c, respectively), simulated ignition delay times are significantly

DOI: 10.1021/acs.jpca.5b00837
J. Phys. Chem. A 2015, 119, 7510−7527

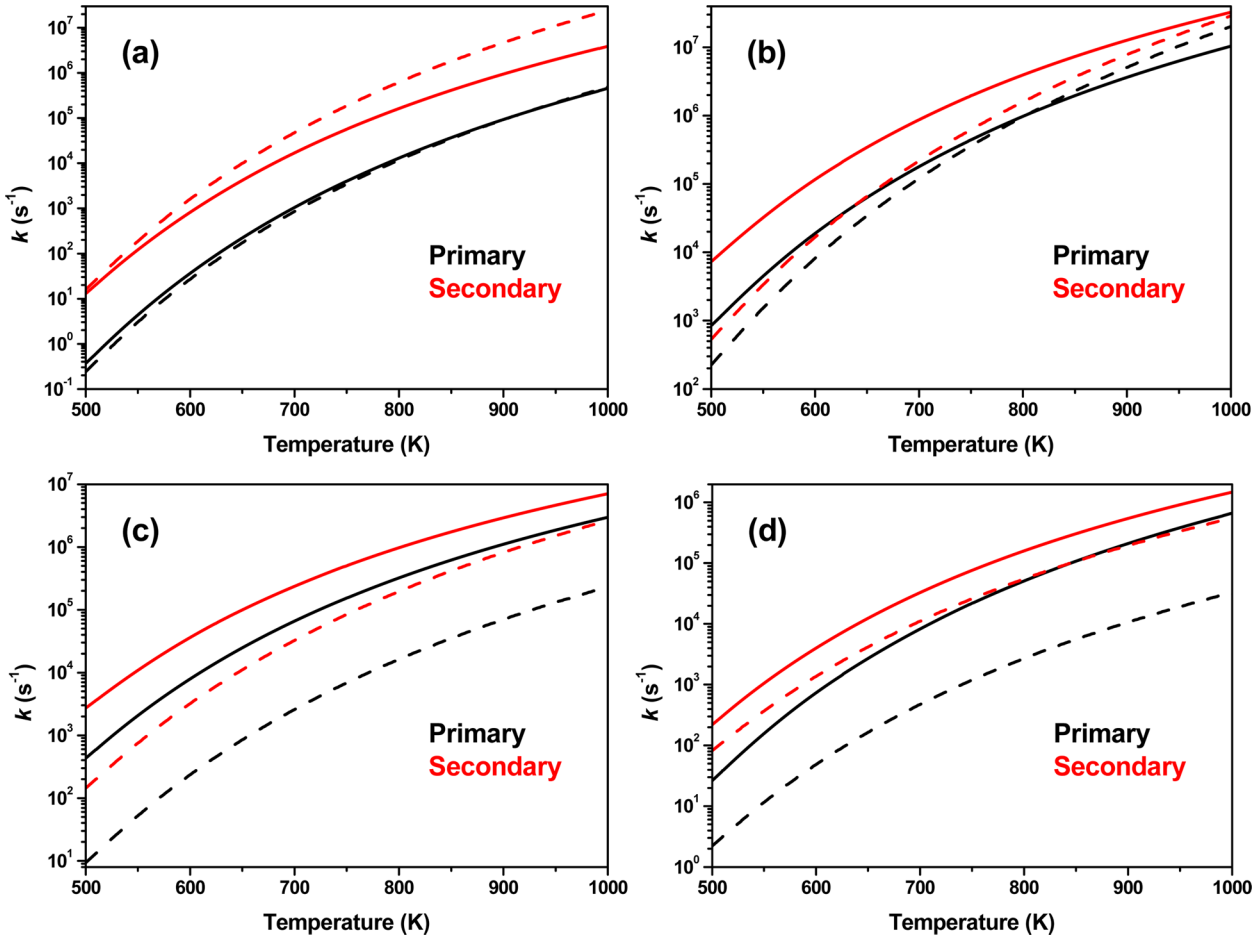

Figure 9. Averaged rate coefficients for reactions of $\dot{O}_2QOOH \rightleftharpoons$ carbonyl-hydroperoxide + $\dot{O}H$ progressing through (a) 5-, (b) 6-, (c) 7-, and (d) 8-membered TS rings. Solid lines correspond to Miyoshi[16] and dashed lines correspond to Sharma et al.[17]

longer when applying the directly calculated rate coefficients of Sharma et al. to the first and second isomerization reactions of *iso*-pentane (Figure 10b). When facility effects are included (i.e., ignition delay times are simulated using non-reactive pressure-time profiles from the RCM), it is shown that the model is in very good agreement with the experimental data, as depicted by the dashed lines in Figure 10 (panels a, b, and d).

With a consistent set of rate coefficients for both *n*-pentane and *iso*-pentane for all of the reaction classes important in the low-temperature regime, it is shown that there is good agreement between the models and their respective experimental targets. Figure 10c illustrates the effects on simulation results of using rate coefficients from Miyoshi[16] and from Sharma et al.[17] for the second isomerization reaction of *neo*-pentane, and it is shown that the model overpredicts reactivity. The low-temperature oxidation mechanism of *neo*-pentane contains a relatively small number of reactions due to its high symmetry. Due to the sensitivity of simulated IDTs to these reactions, the rate coefficients could not be modified within reasonable uncertainty in order to rectify the discrepancy between the model simulations and the experimental measurements. This led us to investigate an anomaly in the stated rate coefficients in the study by Sharma et al.[17] The most similar reaction to that of the second isomerization reaction of the *neo*-pentane $\dot{O}_2QOOH$ species calculated in their study (aside from the one calculated for that specific reaction) is the reaction of $\dot{O}_2CH_2CH_2CH_2OOH$ to produce $HO_2CH_2CH_2CHO + \dot{O}H$. Both reactions proceed through a 6-membered TS ring and break a C−H bond of approximately equal strength. The activation energies differ by less than 2 kcal mol^{-1} in the temperature range of importance for these reactions (Figure 11b), which is less than a factor of 3 in rate coefficient at 750 K, yet the rate coefficients reported by Sharma et al.[17] for these reactions differ by approximately a factor of 40 at 750 K (Figure 11b), and in fact, the activation energy is higher for the reaction of $\dot{O}_2CH_2C(CH_3)_2CH_2OOH$.

Thus, the difference lies in the pre-exponential factors of the rate coefficients which differ by approximately 2 orders of magnitude at 750 K (Figure 11c). The reason for this is not clear upon investigation of the difference in the Gibbs energies of the $\dot{O}_2QOOH$ and the carbonyl-hydroperoxide species for the two reactions (Figure 11d). It seems unusual for there to be such a discrepancy between pre-exponential factors for reactions of such similarity. We find that use of the rate coefficient calculated for $\dot{O}_2CH_2CH_2CH_2OOH \rightleftharpoons HO_2CH_2CH_2CHO + \dot{O}H$ produces favorable results for model simulations when compared to experimental measurements for *neo*-pentane (Figure 10d). Whereas using the rate coefficient calculated for the reaction specific to the *neo*-pentane system results in an overprediction in reactivity which cannot be overcome by reasonable modification of the rate coefficients in the *neo*-pentane submechanism (Figure 10c).

It is shown that using either directly calculated rate coefficients for the second isomerization reactions or using

DOI: 10.1021/acs.jpca.5b00837
J. Phys. Chem. A 2015, 119, 7510−7527

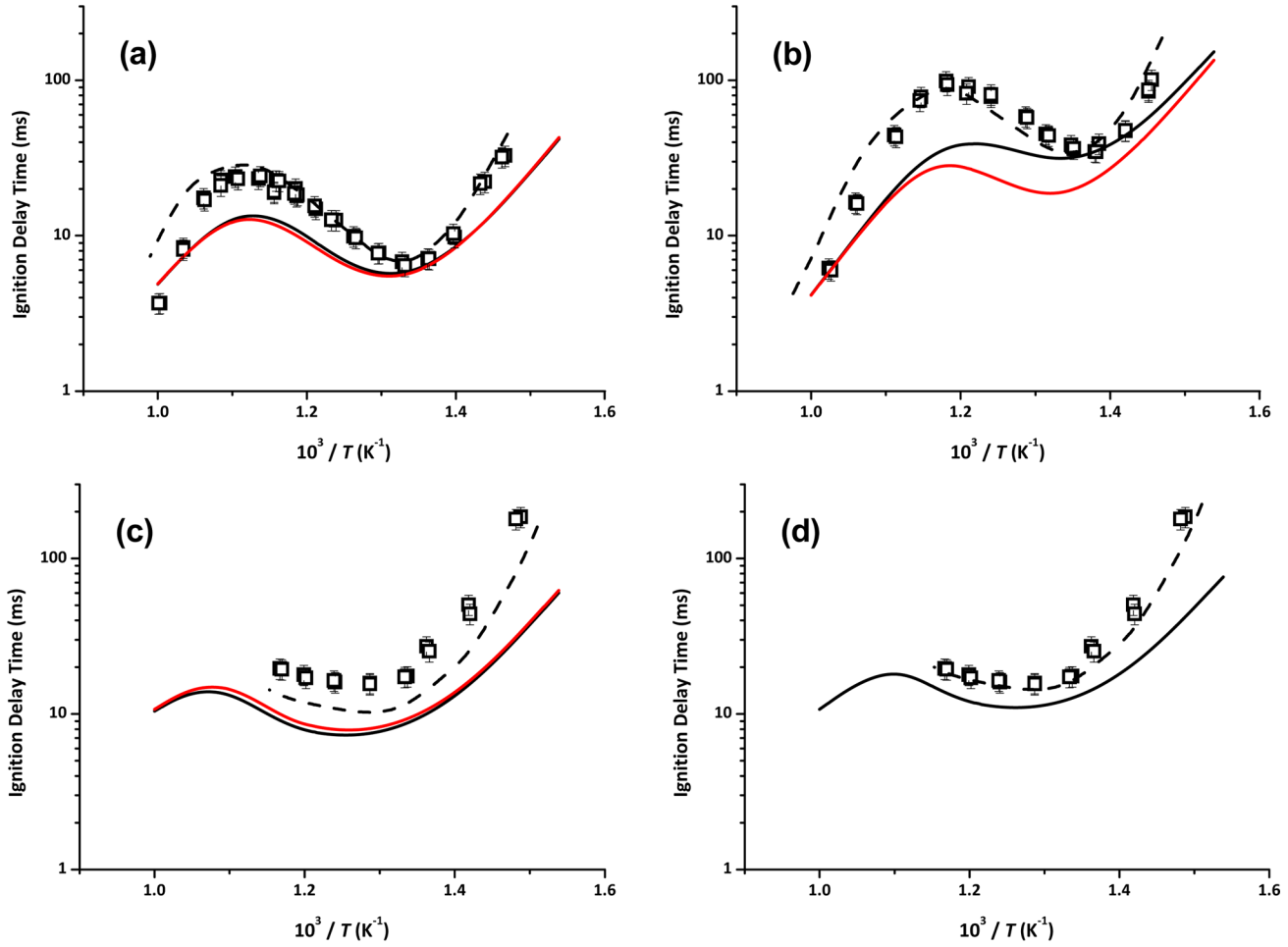

Figure 10. Effect of using calculated rate coefficients for $R\dot{O}_2 \rightleftharpoons \dot{Q}OOH$ and for $\dot{O}_2QOOH \rightleftharpoons$ carbonyl-hydroperoxide + $\dot{O}H$ from (—) Sharma et al.,[17] and (red —) Miyoshi[16] on IDT simulations for (a) *n*-pentane, (b) *iso*-pentane, (c) *neo*-pentane, and (d) *neo*-pentane using a modified second isomerization rate coefficient (described in main text). Dashed lines correspond to model simulated IDTs using the rate coefficients of Sharma et al.[17] and including facility effects. Open symbols represent IDTs for (a) *n*-, (b) *iso*-, and (c and d) *neo*-pentane: all at Φ = 1.0 in "air", 10 atm.

rate coefficients by analogy to the first isomerization reaction class will produce favorable results for *n*-pentane. This is shown not to be the case for *iso*- or *neo*-pentane. The simulated ignition delay time results are far too fast when applying rate coefficients to the second set of isomerization reactions by using an analogy to the first set of isomerization reactions. These findings may provide an explanation to those of Curran et al. in their study of *iso*-octane.[3] In their previous work on *n*-heptane, a set of rate rules was developed which worked well in predicting experimental results.[2] However, they found that when these rules were applied to the *iso*-octane system that reactivity was overpredicted, and in order to match experimental data, the rate coefficients for the isomerization reactions of $R\dot{O}_2$ and of $\dot{O}_2QOOH$ radicals had to be decreased by a factor of 3 relative to their *n*-heptane work. Similar to the findings of this work, it appears that treating the isomerization reactions of $\dot{O}_2QOOH$ radicals by using analogous isomerization reactions of $R\dot{O}_2$ radicals yields good model predictions for the straight-chained species, *n*-pentane, but results in overprediction of reactivity for the branched species, *iso*- and *neo*-pentane. It seems necessary to treat the second isomerization reactions independently of the first, and we find that use of the rate coefficients calculated by Sharma et al.[17] (who propose an alternative treatment when calculating rate coefficients for this complex class of reactions) results in model predictions that match experimental data for both straight- and branched-chained alkanes.

Also investigated were the effects of treating the isomerisations of $\dot{O}_2QOOH$ radicals to produce a carbonyl-hydroperoxide and a hydroxyl radical, as a one- or two-step process (Figure 12). Sharma et al. performed calculations of $\dot{O}_2CH_2CH_2OOH$ producing HO_2CH_2CHO + $\dot{O}H$ at the B3LYP/6-31G(d) level of theory.[17] They found no minima on the potential energy surface for $HO_2CH_2\dot{C}HOOH$. However, when they optimized this intermediate structure at the MP2/CBSB7 level of theory, a minimum was obtained. For *n*-pentane, the formation of a stable α-dihydroperoxyl alkyl radical was allowed, and its decomposition was assigned a low activation energy (1.5 kcal mol^{-1}) due to the instability of the radical. It was found that the effects of adding this intermediate step on simulated IDTs were negligible. We conclude that treating the second isomerization reactions as a single-step process is adequate when constructing chemical kinetic mechanisms. This mirrors the recommendation of Sharma et al.[17]

2.2.3. Alternative $\dot{O}_2QOOH$ Isomerization Reactions. In previous mechanisms,[2,3,20,21] it was assumed that $\dot{O}_2QOOH$ radicals only undergo internal H-atom rearrangements involving the H-atom attached to the carbon which is directly bonded to the OOH group. This is, more often than not, the

DOI: 10.1021/acs.jpca.5b00837
J. Phys. Chem. A 2015, 119, 7510−7527

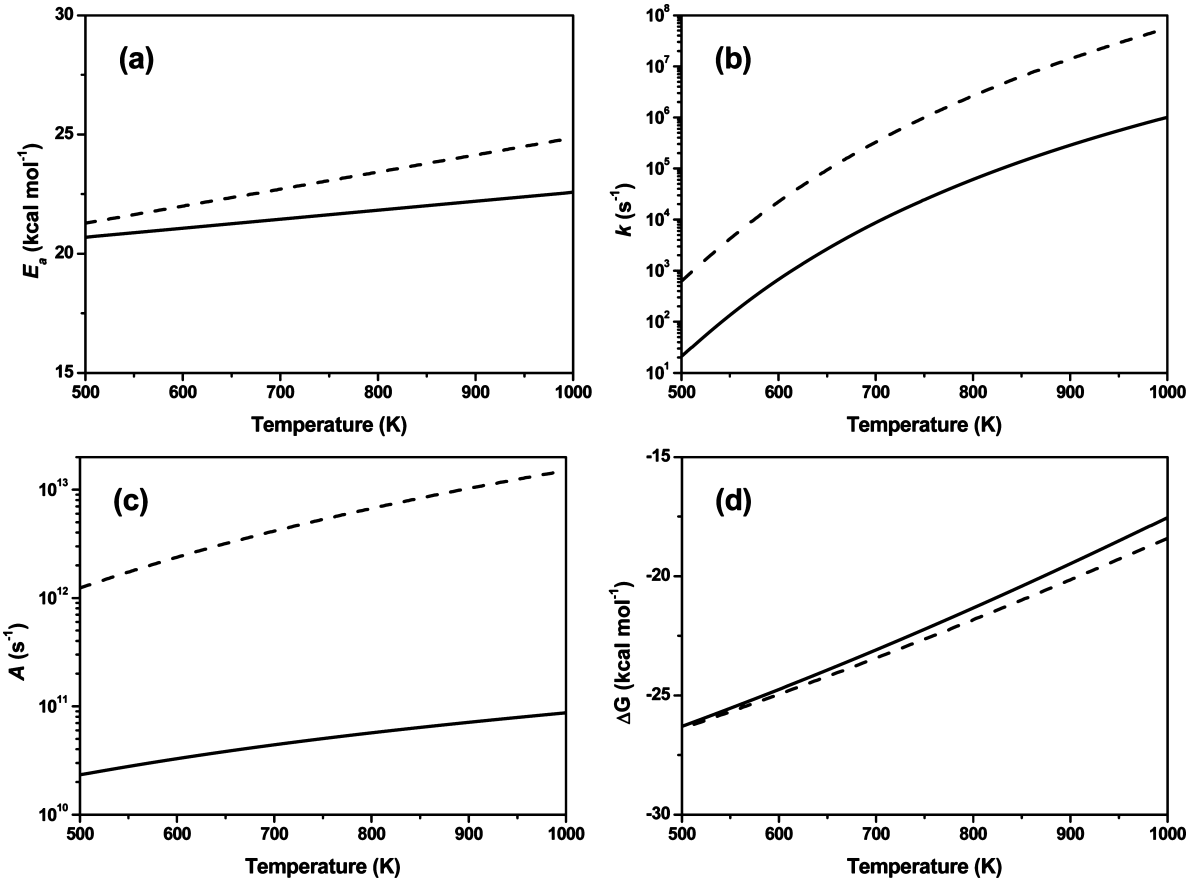

Figure 11. Comparison of (a) activation energies, (b) rate coefficients, (c) pre-exponential factors, and (d) Gibbs energies for the reactions $\dot{O}_2CH_2CH_2CH_2OOH \rightleftharpoons HO_2CH_2CH_2CHO + \dot{O}H$ (solid lines), and $\dot{O}_2CH_2C(CH_3)_2CH_2OOH \rightleftharpoons HO_2CH_2C(CH_3)_2CHO + \dot{O}H$ (dashed lines) from Sharma et al.[17] E_a is calculated from $E_a = E + nRT$, and A is calculated from $A = k/\exp[-(E + nRT)/RT]$, with n and E corresponding to parameters in a typical modified Arrhenius equation; $k = AT^n \exp(-E/RT)$. ΔG is calculated from the thermodynamic parameters used in the study by Sharma et al.,[17] excluding $\dot{O}H$, as the values used in the study are not stated.

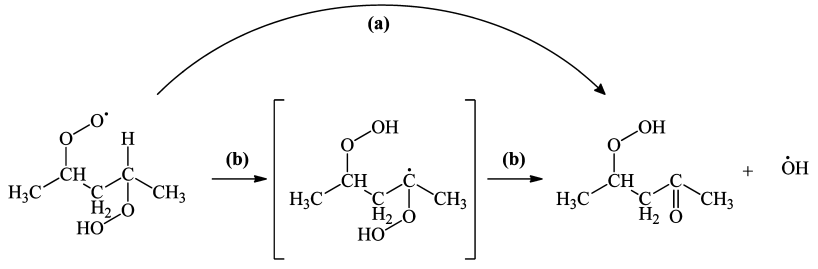

Figure 12. Example reaction of $\dot{O}_2QOOH$ producing carbonyl-hydroperoxide + $\dot{O}H$ treated as (a) a one-step process and (b) a two-step process.

dominant isomerization reaction for these species because the C−H bond is weaker than that of an equivalent C−H bond located on a regular alkyl chain. However, this is not always the case, and in some instances, reactions which compete with these ones can be dominant. Therefore, it is necessary to include these reaction pathways in detailed mechanisms. An example in the *n*-pentane mechanism is the competition between the isomerization reactions of $\dot{O}_2(CH_3)$-$CHCH_2CH_2CH_2OOH$ (Figure 13). The H-shift reaction, which progresses through a 6-membered TS ring, breaking a secondary C−H bond resulting in the formation of a $\dot{P}(OOH)_2$ species (Figure 13b), has a rate coefficient of 1.1×10^6 s^{-1} at 750 K. This is considerably faster than that of the H-shift reaction which proceeds through a 7-membered TS ring, resulting in the formation of a carbonyl-hydroperoxide and a hydroxyl radical (Figure 13a), which has a rate coefficient of 2.3×10^4 s^{-1} at the same temperature.

The main subsequent reaction pathways of the $\dot{P}(OOH)_2$ radicals result in chain branching. Chain branching reactions usually result in an increase in reactivity due to the production of highly reactive radicals. This is found to be the case for some of the reactions of $\dot{P}(OOH)_2$ but not for all of them. The reasons for this will be discussed in the subsequent descriptions of the reaction classes relevant to $\dot{P}(OOH)_2$ radicals.

2.2.4. $\dot{P}(OOH)_2 \rightleftharpoons$ Olefin + $H\dot{O}_2$. These reactions are similar to the *β*-scission reactions of $\dot{Q}OOH$ radicals which also produce an olefin and a hydroperoxyl radical, the rate coefficients of which are used for individual analogous reactions. However, these reactions result in the formation of an olefinic hydroperoxide. Silke[9] found that inclusion of this

DOI: 10.1021/acs.jpca.5b00837
J. Phys. Chem. A 2015, 119, 7510−7527

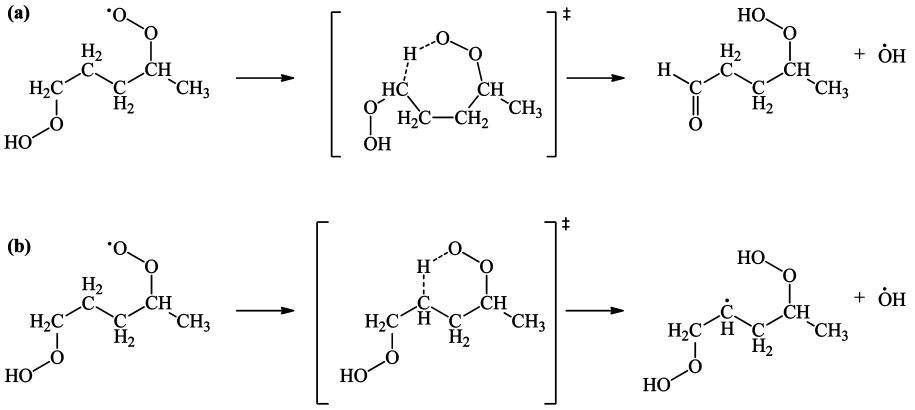

Figure 13. Example reaction of $\dot{O}_2QOOH$ proceeding through (a) a 7-membered TS ring, forming a carbonyl-hydroperoxide + $\dot{O}H$ and (b) a 6-membered TS ring, forming a $\dot{P}(OOH)_2$ species.

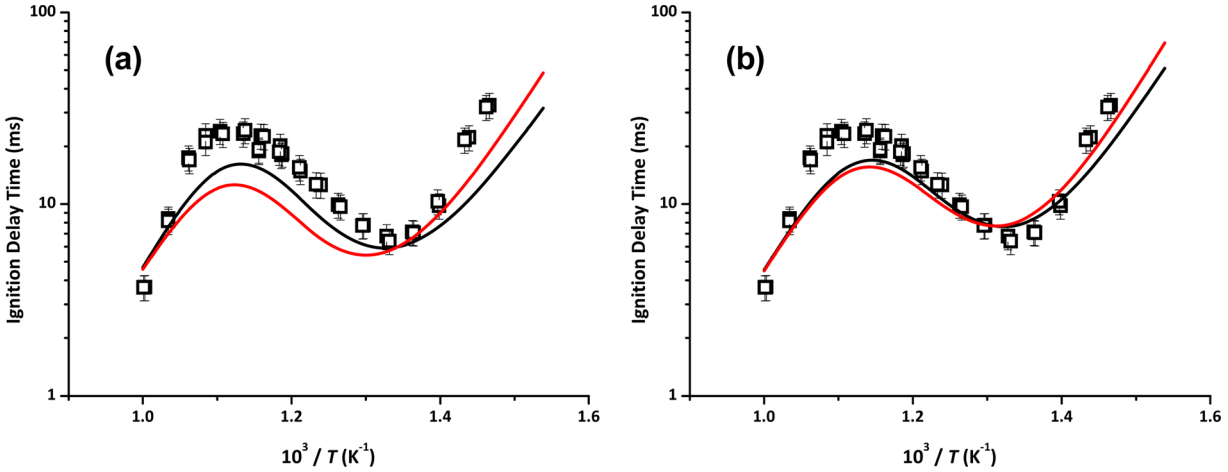

Figure 14. Effect of "alternative" isomerisations of $\dot{O}_2QOOH$. (—) Model before addition of "alternative" isomerisations. (red —) Model including "alternative" isomerization reactions. Open symbols represent ignition delay times for *n*-pentane, Φ = 1.0 in "air", 10 atm, acquired over the course of this study. (a) c5_49 model.[20] (b) This work.

reaction class in an *n*-heptane mechanism resulted in an increase in reactivity at temperatures above ~830 K and a decrease in reactivity at temperatures below this (Figure 4a). Inclusion of this reaction class to the mechanism developed by Healy et al.[20] (c5_49) results in a similar effect for *n*-pentane, although it is less pronounced, but still significant (Figure 14a). However, when this reaction class is added to the *n*-pentane mechanism developed in this study, the effect of these alternative isomerization reactions is minimal (Figure 14b). A reduction in reactivity at lower temperatures (below ~770 K) and an increase at higher (~770−900 K) is seen, but the changes in equilibria brought about by the thermochemistry updates have caused these pathways to be virtually insignificant in their contribution to overall reactivity.

The subsequent decomposition of the olefin occurs via fission of the O−O bond in the hydroperoxide group, resulting in the production of a hydroxyl radical. The reaction sequence constitutes chain branching because a hydroxyl and a hydroperoxyl radical are produced from the original $\dot{P}(OOH)_2$ species, along with an olefinic alkoxy radical species. However, before inclusion of this reaction class, two hydroxyl radicals and a carbonyl alkoxy radical species would have been produced. Previously, the only pathway considered for $\dot{O}_2QOOH$ radicals were isomerization reactions to form a carbonyl-hydroperoxide and a hydroxyl radical, followed by decomposition of the carbonyl-hydroperoxide, resulting in the production of a second hydroxyl radical. The production of a hydroperoxyl radical rather than a second hydroxyl radical leads to the reduction in reactivity at the lower temperature portion of the negative temperature coefficient (NTC) region, and conversely, the increase in reactivity at higher temperatures. This is because H-atom abstraction from the parent fuel molecule by hydroxyl radicals is orders of magnitude faster than that by hydroperoxyl radicals, and is also far more exothermic, with $\Delta\Delta H_{rxn} = -31.8$ kcal mol^{-1} at 750 K, where $\Delta\Delta H_{rxn}$ is calculated from $\Delta\Delta H_{rxn} = \Delta H_{rxn}$(H atom abstraction by $\dot{O}H$) − ΔH_{rxn}(H atom abstraction by $H\dot{O}_2$). This explains the decrease in reactivity at lower temperatures, as the relative concentrations of hydroperoxyl to hydroxyl radicals are increased with the inclusion of this reaction class. However, this shift in the relative concentrations becomes favorable from a reactivity standpoint at higher temperatures, due to the H_2O_2 produced from H-atom abstraction by hydroperoxyl radical being able to overcome the relatively high barrier (~48.7 kcal mol^{-1})[30] for unimolecular decomposition, to form two highly reactive hydroxyl radicals.

2.2.5. $\dot{P}(OOH)_2 \rightleftharpoons$ Cyclic Ether + $\dot{O}H$. These reactions are analogous to those of $\dot{Q}OOH$ radicals which form cyclic ethers and $\dot{O}H$ radicals. The decomposition of the hydroperoxyl cyclic ether formed in these reactions results in the production of a

DOI: 10.1021/acs.jpca.5b00837
J. Phys. Chem. A 2015, 119, 7510−7527

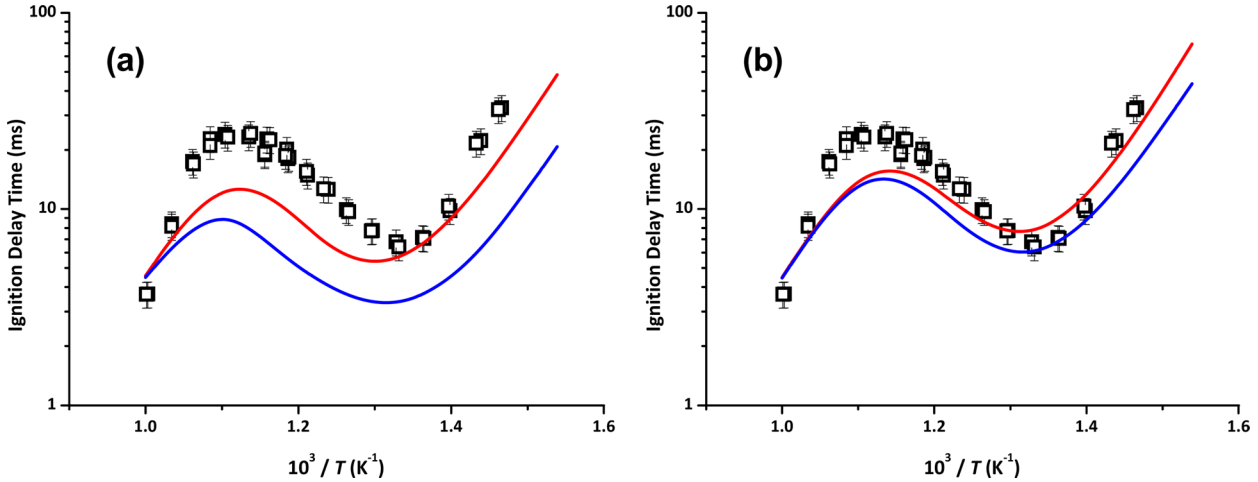

Figure 15. Effect of hydroperoxyl cyclic ether formation from $\dot{P}(OOH)_2$. (red —) Model including "alternative" isomerization reactions. (blue —) Model including "alternative" isomerization reactions and hydroperoxyl cyclic ether formation. Open symbols represent ignition delay times for *n*-pentane, Φ = 1.0 in "air", 10 atm, acquired over the course of this study. (a) c5_49 model.[20] (b) This work.

second hydroxyl radical. This chain branching is similar to that of the "traditional" second isomerization reactions which proceed through a carbonyl-hydroperoxide species. This explains the increase in reactivity observed upon inclusion of this reaction class across the majority of the temperature range investigated by Silke[9] in the study of *n*-heptane (Figure 4b).

Figure 15 illustrates the effect of inclusion of the $\dot{P}(OOH)_2 \rightleftharpoons$ cyclic ether + $\dot{O}H$ pathways to c5_49[20] and to the mechanism presented in this study. The reactivity promoting effect observed by Silke upon inclusion of this reaction class to the mechanism of *n*-heptane[9] is also observed for *n*-pentane for both mechanisms investigated, although the effect is confined to lower temperatures (below ∼1000 K). As is observed with the alternative isomerization reactions (Figure 14), the addition of the hydroperoxyl cyclic ether pathways has a more pronounced effect on the mechanism of Healy et al.[20] than on the mechanism presented herein (Figure 15). Again, this is due to the lower relative flux to these pathways brought about by equilibrium changes induced by the updated thermochemical values.

2.2.6. Additional Pathways. In addition to the aforementioned pathways, concerted elimination reactions from $\dot{O}_2QOOH$ radicals directly producing olefinic hydroperoxides and $H\dot{O}_2$ (analogous to the concerted elimination reactions of $R\dot{O}_2$) were included in the mechanisms of *n*- and *iso*-pentane. As is the case with the concerted elimination reactions of $R\dot{O}_2$, this additional pathway is not possible in the *neo*-pentane reaction scheme, as there are no C−H bonds beta- to the peroxyl moiety in either the *neo*-pentyl peroxyl or the hydroperoxyl *neo*-pentyl peroxyl radicals. The inclusion of this class of reactions to the *n*- and *iso*-pentane mechanisms had little effect on IDT simulation results.

Ranzi et al.[31] and Pelucchi et al.[32] have recently investigated the importance of new reaction classes in modeling the low-temperature oxidation of *n*-alkanes. These investigations were undertaken in light of recent experimental data detailing several intermediate species produced from the low-temperature oxidation of propane, *n*-butane, and *n*-heptane, using advanced analytical techniques.[33−38] These oxygenated intermediates include ketones, diones, and organic acids, and are formed primarily at quite low temperatures (<650 K). The reaction classes investigated were (1) H-atom abstractions from alkyl and carbonyl-hydroperoxides, (2) unimolecular reactions of carbonyl-hydroperoxides forming organic acids via the Korcek mechanism,[39] and (3) recombination/disproportionation reactions of peroxyl radicals. It was found that inclusion of these reaction classes had minimal effect on model predictions of overall reactivity but was advantageous in simulating the concentration−temperature profiles of the aforementioned oxygenated intermediates. While these pathways have not been included in the mechanisms of the pentane isomers, the findings of Ranzi et al. and Pelucchi et al. suggest that inclusion of these pathways will not have a significant effect on current model predictions of reactivity.[31,32] Indeed, Pelucchi et al. show that, at 650 K, 94% of C_7 carbonyl-hydroperoxides decompose via simple fission of the O−O bond in the hydroperoxyl group.[32] In light of this, we find it adequate to describe the decomposition of C_5 carbonyl-hydroperoxides via unimolecular decomposition alone, given the temperature range of the experiments (>640 K) over which the mechanisms have been validated.[19] However, should speciation data become available for the pentane isomers in the low-temperature regime, inclusion of these pathways should be facile.

2.2.7. Pressure Dependence. Unimolecular decomposition reactions of the parent fuel molecule are important at high temperatures (>1200 K), where deviation by rate coefficients from the high-pressure limit can be non-negligible. These reactions have been treated as being pressure-dependent in this study for the pentane isomers, even though the effect of this treatment was not found to be significant in simulating ignition delay times at the temperatures investigated in this study. High-pressure limit rate coefficients were calculated through microscopic reversibility using estimates for radical−radical recombination reactions and utilizing the CHEMRev software package.[40] Pressure dependent rate coefficients were calculated using Quantum-Rice-Ramsperger-Kassel/Modified Strong Collision (QRRK/MSC) theory. Lennard-Jones parameters of σ = 4.23 Å and ε = 192 cm^{-1} were used in these calculations for *n*-pentane in N_2 bath gas and are obtained from the work of Jasper and Miller.[41] Lennard-Jones parameters for both *iso*- and *neo*-pentane were not calculated in the aforementioned study and so were assumed to be the same as those for *n*-pentane. Pelucchi et al. demonstrate the applicability of the QRRK/MSC method for reactions of this kind through comparison with the

DOI: 10.1021/acs.jpca.5b00837
J. Phys. Chem. A 2015, 119, 7510−7527

Table 2. Recommended Rate Rules

$\dot{R} + O_2 \leftrightarrow R\dot{O}_2$					
addition site	A (cm^3 mol^{-1} s^{-1})	n	E (cal mol^{-1})	uncertainty (upper, lower)	refs[a]
primary	1.301×10^{11}	0.230	−1580	1.7, 2.2	12, 14, 15, 49−54
secondary	1.507×10^{15}	−0.920	−130	2.1, 1.7	12, 14, 15, 49, 53
tertiary	2.464×10^{11}	0.400	−800	1.4, 1.7	12, 14
$R\dot{O}_2 \leftrightarrow$ Olefin + $H\dot{O}_2$					
	A_H (s^{-1})	n	E (cal mol^{-1})	uncertainty (upper, lower)	refs
	2.885×10^{09}	0.930	29800	2.8, 2.2	12, 16
$R\dot{O}_2 \rightleftharpoons \dot{Q}OOH$[b]					
subclass	A_H (s^{-1})	n	E (cal mol^{-1})	uncertainty (upper, lower)	refs
1,4p	2.563×10^{12}	−0.130	34360	2.4, 2.3	12, 16, 17
1,4s	2.327×10^{07}	1.400	28660	4.2, 3.1	12, 16, 17
1,4t	5.629×10^{10}	0.330	26700	1.9, 2.0	12, 16, 17
1,5p	5.869×10^{08}	0.780	21850	2.5, 2.7	12, 16, 17
1,5s	8.204×10^{10}	0.130	19470	2.2, 2.3	12, 16, 17
1,5t	1.819×10^{07}	1.190	15000	2.1, 2.0	12, 16, 17
1,6p	2.063×10^{07}	1.000	21070	1.8, 1.7	12, 16, 17
1,6s	7.054×10^{08}	0.510	17600	1.6, 2.3	12, 16, 17
1,6t	1.287×10^{07}	0.960	14290	1.5, 1.6	12, 16, 17
1,7p	2.968×10^{07}	0.800	21400	1.2, 1.2	12, 16, 17
1,7s	1.143×10^{10}	0.040	19780	1.4, 3.6	12, 16, 17
1,7t	2.956×10^{09}	0.040	16350	1.2, 1.3	12, 16, 17
$\dot{Q}OOH \leftrightarrow$ Olefin + $H\dot{O}_2$					
	A (s^{-1})	n	E (cal mol^{-1})	uncertainty (upper, lower)	refs
β-$\dot{Q}OOH$	1.829×10^{10}	0.790	15100	2.4, 3.3	13, 16
$\dot{Q}OOH \leftrightarrow$ Cyclic Ether + $\dot{O}H$					
subclass	A (s^{-1})	n	E (cal mol^{-1})	uncertainty (upper, lower)	refs
β-$\dot{Q}OOH$	2.282×10^{08}	1.290	9890	3.4, 3.3	13, 16
γ-$\dot{Q}OOH$	4.579×10^{15}	−1.080	18440	35.8, 11.1	13, 16
δ-$\dot{Q}OOH$	3.502×10^{10}	0.100	9330	7.4, 6.2	13, 16
ε-$\dot{Q}OOH$	3.553×10^{07}	0.690	10970	4.3, 4.0	13, 16
$\dot{Q}OOH \leftrightarrow \beta$-Scission Products[c]					
subclass	A (s^{-1})	n	E (cal mol^{-1})	uncertainty (upper, lower)	refs
γ-$\dot{Q}OOH$	5.819×10^{05}	2.400	22790	8.5, 6.0	13, 16
δ-$\dot{Q}OOH$	2.740×10^{13}	0.240	29830	2.7, 1.8	13, 16

[a]Rate coefficients from the references listed were considered in deriving the recommended rate rules. [b]Subclass nomenclature represents the number of non-hydrogen atoms in the transition state ring structure, followed by the type of H atom being abstracted: p, s, and t = primary, secondary and tertiary, respectively [e.g., 1,4p refers to an isomerization proceeding through a 5-membered TS ring (4 non-hydrogen atoms), and breaking a primary C−H bond]. [c]In this reaction class, γ-$\dot{Q}OOH$ refers to the reactions of those species which undergo concerted C−C/O−O bond fission. δ-$\dot{Q}OOH$ refers to the reactions of those species which undergo C−C bond fission to produce an olefin and a β-$\dot{Q}OOH$.

more rigorous Rice-Ramsperger-Kassel-Marcus/Master Equation (RRKM/ME) approach and show that there is good agreement between both sets of computations for the unimolecular decomposition reactions of alkanes.[42]

Several shock tube studies[43−45] were performed at the National Institute of Standards and Technology (NIST) and the University of Illinois at Chicago (UIC), investigating the decomposition of pentyl radicals over a wide range of temperatures (833−1130 K) and pressures (0.8−50 bar). High-pressure rate expressions for H-transfer reactions and β-scissions were derived, and RRKM/ME analyses were performed and used to extrapolate the data in the temperature range of 700−1900 K, at pressures of 0.1−1000 bar. The effect of using pressure-dependent rate coefficients, as opposed to the high-pressure limit rate coefficients, was investigated for *n*-pentane in this study. It was found that the effect was negligible on ignition delay time simulation results at the pressures and over the temperature range investigated here. Although the pressure dependence of pentyl radical decomposition was found to have a negligible effect on ignition delay simulations, the pressure-dependent rate coefficients have been retained in the current mechanism to allow future development for validation against speciation (more specifically, pyrolysis) data, as the various studies at NIST and UIC found that major product ratios can vary significantly with pressure.

Villano et al.[12,13] investigated the effect of pressure for representative small (n-$\dot{C}_4H_9$), medium (n-$\dot{C}_8H_{17}$), and larger (n-$\dot{C}_{12}H_{25}$) alkyl radical plus O_2 reactions over a wide range of temperatures and pressures using the QRRK/MSC method. Comparisons of product concentration−time profiles using two mechanisms (one that used pressure-dependent rate coefficients and one that used the corresponding high-pressure limit values) were made to observe the effect of pressure. For most of the conditions investigated, it was found that the predictions with both mechanisms were similar in terms of the predicted final product distributions, even though in some instances there

DOI: 10.1021/acs.jpca.5b00837
J. Phys. Chem. A 2015, 119, 7510−7527

were differences in the early time profiles. Small differences in the steady-state product distributions occurred at high temperatures (1000 K) and low pressures (0.1 atm). The largest differences occurred for the reaction of *n*-butyl radical with O_2. The predictions of the two mechanisms for all of the radicals investigated were in good agreement at 10 atm, suggesting that under typical combustion/ignition conditions, high-pressure limit rate coefficients can be used directly to describe low-temperature oxidation chemistry without any further consideration of pressure effects. Recent studies by Burke et al.[46] and Goldsmith et al.[47] on the *n*-propyl low-temperature oxidation system also suggest that pressure-dependent effects may become greatly diminished at pressures above 1 atm. With the low-temperature reactions of *n*-propyl and *n*-butyl radicals not exhibiting significant pressure-dependent effects under the conditions investigated by Villano et al.,[12,13] Burke et al.,[46] and Goldsmith et al.,[47] we expect the reactions of the larger alkanes to show even less dependence on pressure. Due to these findings, we have described the low-temperature oxidation reactions of the pentane isomers using high-pressure limit rate coefficients.

3. RECOMMENDED RATE RULES

Recommended rate rules for reaction classes have been developed based on a review of rate coefficients in the literature. This will offer the broadest possible scope of existing rate coefficients for reactions relative to the low-temperature oxidation of alkanes that are in the literature and the level of uncertainty in them and will provide chemical kinetic modellers with a useful tool in the development of mechanisms for large hydrocarbons. It should be noted that, where possible, rate coefficients from the literature that were calculated for the reactions specific to the pentane isomers have been used in the mechanisms presented in this work. The rate rules discussed herein are not those used in the mechanisms of the pentanes but are instead here for use in the mechanisms of larger alkanes for which calculations do not exist for their specific reactions. Rate rules made for this purpose have been developed by calculation of high-pressure limit rate coefficients for many reactions relevant to the low-temperature oxidation of alkanes (straight- and branched-chained) in several recent studies.[12−14,16,17] However, in this work, we aim to develop new rate rules, taking into account the rate coefficients calculated in all of these studies, as well as from others, which have used various levels of quantum theory to obtain their respective results.

The rate coefficients considered for development of the rate rules were compared over a temperature range of 500−1250 K (in 50 K increments). This covers the range over which all of the rate coefficients have been calculated in their respective studies. In all, 344 rate coefficients were considered in the development of the 23 rate rules shown in Table 2. In order to remove outliers (which would otherwise skew rate rule estimations and lead to higher uncertainties) upper and lower limits were defined. The upper limit was defined as the third quartile plus 1.5 times the interquartile range of the rate coefficients considered for each reaction class/subclass. The interquartile range was defined inclusive of the median, where applicable. The lower limit was defined as the median divided by the factor difference between the upper limit and the median. Any rate coefficients outside of the defined limits were excluded when developing the rate rule for each reaction class/subclass. An example of this is illustrated in Figure 16.

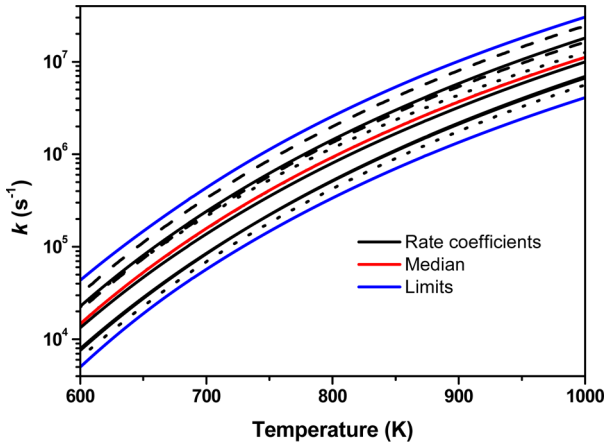

Figure 16. Example of rate rule determination for 1,5s subclass of $R\dot{O}_2 \rightleftharpoons \dot{Q}OOH$ reaction class. Solid lines correspond to Villano et al.,[12] dashed lines correspond to Miyoshi,[16] and dotted lines correspond to Sharma et al.[17]

The resulting median was fitted to the following modified Arrhenius expression:

$$k = AT^n \exp(-E/RT)$$

where A is the A-factor, n is the temperature exponent, and E is related to the activation energy (by $E_a = E + nRT$). A_H in Table 2 is the A-factor expressed on a per H-atom basis. The stated uncertainties for each of the rate coefficients in Table 2 represents the largest factor difference between the rate rule and each individual rate coefficient considered in the rate rule estimation for that specific reaction class/subclass once outliers are removed. It should be noted that the rate coefficients utilized in the rate rule estimations each have their own inherent uncertainties arising from errors within the various ab initio methods used to calculate them.

As an aid to kinetic modellers, both upper and lower uncertainties are given, as opposed to a single uncertainty factor which assumes an even level of upper and lower bounds. These upper and lower uncertainties are defined according to

$$\text{upper uncertainty} = k_{max}/k_{rule,}$$

$$\text{lower uncertainty} = k_{rule}/k_{min}$$

where k_{rule} refers to the derived rate rule, k_{max} the maximum rate coefficient used in the rate rule estimation, and k_{min} the minimum rate coefficient used in the rate rule estimation. Here it is assumed that a rate coefficient is uniformly distributed within its uncertainty bounds (i.e., its uncertainty is assumed to be temperature-independent). The use of other distributions is possible but is beyond the scope of this study. However, statement of upper and lower uncertainties will allow modellers to have a more refined scope for reasonable modification of rate coefficients for optimization toward experimental targets. As stated in the recent study by Cai and Pitsch,[48] when optimizing a mechanism, it is not reasonable to modify individual rate coefficients within a reaction class just because it shows a higher sensitivity than other reactions in the same class, as this leads to inconsistency within a mechanism, and results in kinetically similar reactions being treated differently. This is especially true when constructing large mechanisms, for which the recommended rate rules presented in this work are designed for use. It is recommended that the rate rules developed here be

DOI: 10.1021/acs.jpca.5b00837
J. Phys. Chem. A 2015, 119, 7510−7527

modified rather than individual reaction rate coefficients, unless information is otherwise available for a particular reaction from experimental measurements or ab initio calculations.

To our knowledge, the studies by Goldsmith et al.[15] on the propyl + O_2 system, and Zádor et al.[29] on 2-hydroperoxyl-2-methylprop-1-yl + O_2, are the only studies which present rate coefficients for $\dot{Q}OOH$ addition to O_2 based on experimental or theoretical results. For this reason, rate rules have not been developed here for this reaction class. It should be noted that (as mentioned previously) these rate coefficients have not been used in the mechanisms of the pentane isomers in this work.

Rate coefficients for the isomerization reactions of $\dot{O}_2QOOH$ producing carbonyl-hydroperoxide + $\dot{O}H$ have been calculated by both Miyoshi[16] and Sharma et al.[17] Rate rules have not been derived for this reaction class for two main reasons: (1) there are a low number of calculated rate coefficients available for this reaction type, and (2) the groups of rate coefficients which have been calculated in both studies are systematically different from one another (Figure 9). In modeling the pentane isomers, we find that the rate coefficients calculated by Sharma et al.[17] best reproduce the experimental data for all of the isomers. Consequently, we recommend the rate coefficients calculated by Sharma et al. for reactions of this type, which were developed for archetypal reactions and can be used as rate rules for mechanisms of large hydrocarbons.[17]

Figure 17 shows a comparison between the original rate rule[3] for the 1,5s subclass of the $R\dot{O}_2 \rightleftharpoons \dot{Q}OOH$ reaction class and

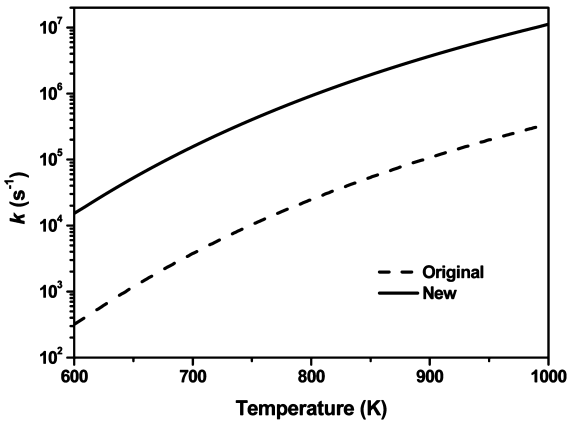

Figure 17. Rate rule comparison for 1,5s subclass of $R\dot{O}_2 \rightleftharpoons \dot{Q}OOH$ reaction class. Dashed line corresponds to original rate rule.[3] Solid line corresponds to new rate rule.

the one recommended in this work. There is a difference of approximately a factor of 40 at 750 K. This magnitude of difference (and sometimes more) is observed for several of the reaction classes listed in Table 2. This illustrates the significance of the change brought about by the improvement in, and implementation of, computational methods employed to the low-temperature oxidation kinetics of alkanes. Yet, there is still a high level of uncertainty in many rate coefficients, even when calculated at a similar level of theory by several research groups. There is need for a more thorough investigation of an individual system (such as *n*-pentane) at higher levels of theory in order to refine our understanding of low-temperature oxidation systems.

4. RESULTS AND DISCUSSION

RCM experiments were simulated using the closed homogeneous batch reactor module in CHEMKIN-PRO.[55] For the simulation of RCM experiments, the calculations use volume profiles generated from non-reactive pressure traces. The volume history is used to simulate reaction during the compression stroke and the heat losses that occur during the experiments.

Figure 18 shows comparisons of the pentanes model with RCM data for each of the isomers, alongside mechanisms using

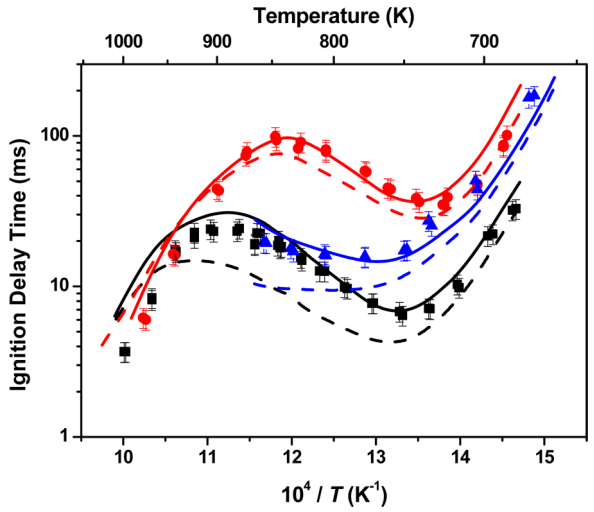

Figure 18. Comparison of mechanisms using rate coefficients for specific pentane reactions versus mechanisms using the rate rules recommended in this work. Black symbols and lines represent *n*-pentane, red represents *iso*-pentane, and blue represents *neo*-pentane. Dashed lines correspond to "rate rule mechanisms". Solid lines correspond to the mechanisms proposed in this work. All simulations shown have included facility effects. Φ = 1.0 in "air". p_C = 10 atm.

the recommended rate rules from Table 2. The rate rules have been employed to all of the reaction classes listed in Table 2, as well as the alternative pathways, as the rate coefficients used for these pathways come from analogy to those listed in Table 2. The rate coefficients for the second additions to O_2 in the "rate rules mechanisms" have been reduced by a factor of 2 relative to their analogous first addition to O_2, in accordance with what has been done in the validated mechanisms. First, it is seen that there is excellent agreement between the mechanisms which use pentane-specific rate coefficients and the experimental data. And second, it is shown that there is agreement between these mechanisms and the "rate rules mechanisms" within a factor of 2 across the temperature range shown. This bodes well for future application of the rate rules to mechanisms of larger alkanes as they perform well for the straight-chained and branched-chained fuels. For the cases shown in Figure 18, optimization of the mechanisms would require minimal effort, due to the models' proximity to the experimental data and the fact that there are 23 modifiable rate rules to work with.

However, this further illustrates the level of uncertainty that still exists in the rate coefficients for the important low-temperature reactions. For a given set of thermochemical values there are still many ways to achieve good agreement between model simulations and experimental targets, by modifying either rate coefficients for elementary reaction steps or rate rules for reaction classes, within their respective uncertainty

DOI: 10.1021/acs.jpca.5b00837
J. Phys. Chem. A 2015, 119, 7510−7527

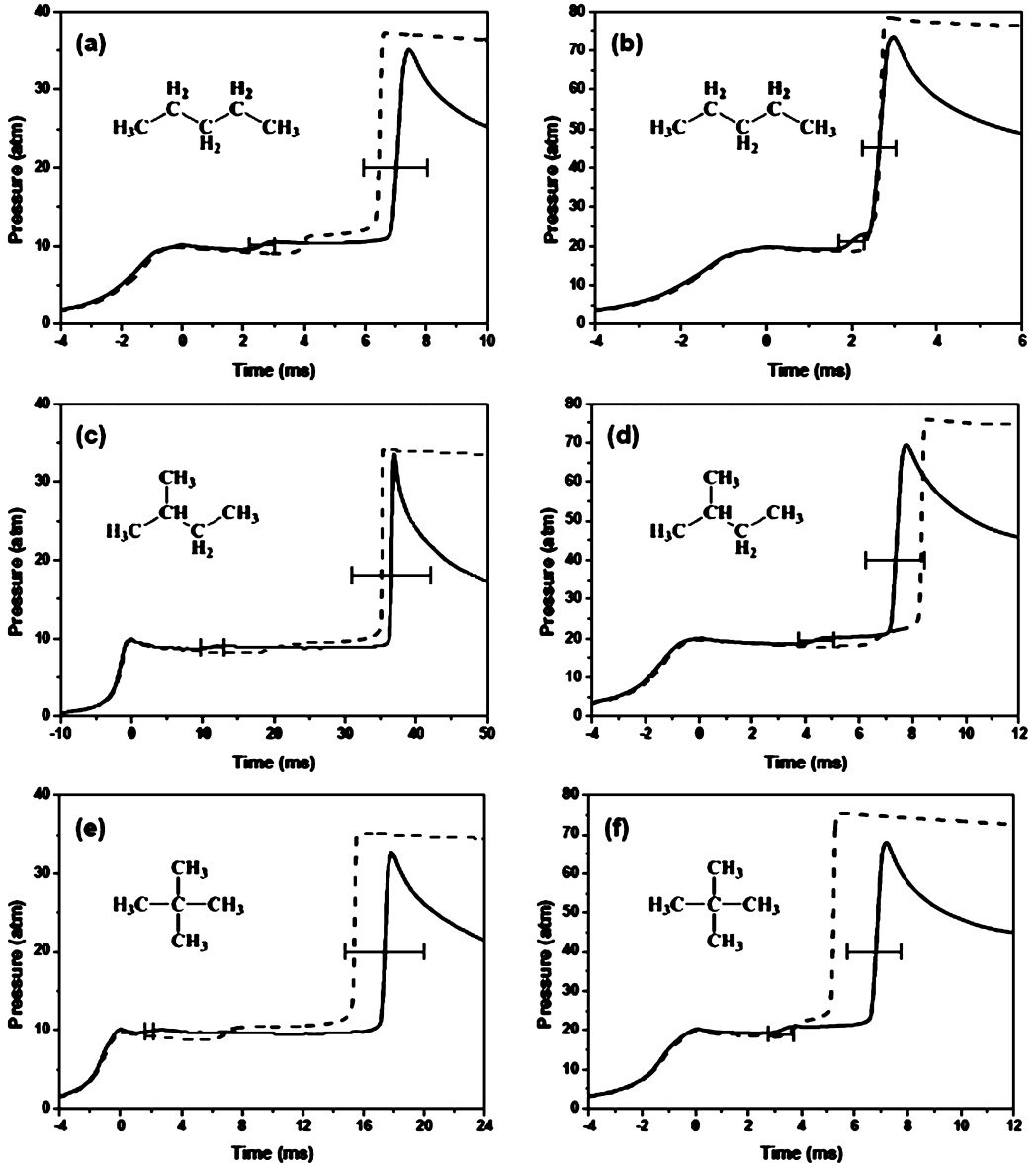

Figure 19. Comparison of experimental and simulated pressure-time histories. Φ = 1.0 in "air". Diluent = 100% N_2. T_C range: 734−753 K. (a, c, and e): $p_C \approx 10$ atm. (b, d, and f): $p_C \approx 20$ atm. Solid lines represent experiments. Dashed lines represent simulations (using volume history from RCM). Fifteen percent error bars are included on both first- and second-stage ignition delay times.

bands. Further updates to thermochemical group values pertinent to species important in the low-temperature regime would likely require reoptimization of kinetic parameters. A semi-automated system, such as that demonstrated by Cai and Pitsch,[48] provides an efficient and sensible approach to mechanism optimization, by using rate rules as optimizable parameters within stated uncertainty bounds. Updating of rate rules and their uncertainties based on emerging literature values and utilizing the statistical approach employed in this study, respectively, coupled with a system such as that used by Cai and Pitsch, may provide a dynamic approach for future model optimization.

Figure 19 shows comparisons of model simulations with experimental pressure-time histories for each of the isomers at 10 and 20 atm, over a similar range of temperatures. The temperatures of the experiments shown in Figure 19 were chosen to allow comparison of the model with data that exhibit two clear ignition events, as low-temperature oxidation chemistry plays a key role in this two-stage ignition phenomenon. There is very good agreement between the model and experimental data for these cases, with first and second stage IDTs well predicted. The pressure rise due to first-stage ignition is slightly overpredicted by the model, as is to be expected when using a zero-dimensional modeling approach for a multi-stage ignition situation.[56,57] Various methods[58,59] beyond the scope of this study could be utilized in order to improve agreement with first-stage ignition pressure rise, and second-stage ignition delay times, but the benefits, in terms of the aims of this study, would be minimal considering the relatively minute discrepancies between the model and the experimental data.

Further validation and analysis of the mechanisms will be presented in an accompanying paper.[19]

DOI: 10.1021/acs.jpca.5b00837
J. Phys. Chem. A 2015, 119, 7510−7527

5. CONCLUSIONS

There have been significant changes to the thermochemical properties values and rate coefficients for the species and reactions important to low-temperature oxidation, respectively. By using the most up-to-date thermochemistry group values and rate coefficients from several recent publications, the current model shows very good agreement with experimental data. We show that revisions to both the thermochemistry and the kinetics are required in order to replicate experiments well.

Past models that used the rate rule estimates of Curran et al.[2,3] for reaction classes, replicated experimental data very well. However, it would seem that this is due to a series of compensating errors in terms of both thermochemistry and rate coefficient assignments, which may have been overcome in certain instances by not allowing thermochemical equilibrium to hold (i.e., by definition of rate coefficients in both the forward and reverse directions). Previous thermochemistry generated utilizing group additivity rules used by Curran et al. most likely hindered a more accurate estimation of rate rules for the reaction classes. This work represents a major change in the understanding of the low-temperature oxidation of alkanes and shows that careful consideration of both thermochemistry and rate coefficients is essential in order to accurately replicate experimental data.

Additional reaction classes have been considered but have not had a large influence on model predictions, which is in contrast to that observed by Silke.[9] It is important that these reaction pathways are included in alkane (and other fuel types) reaction mechanisms, as detailed chemistry gives a precise picture of *all* of the reactions controlling the various stages of combustion, and is imperative for a detailed understanding of various fuel behavior and model predictions in a multitude of combustion systems. The reason for the less significant effect of the additional classes on model predictions is likely a result of the use of more accurate thermochemistry values and rate coefficients compared to those used previously. The updated thermochemistry values have changed equilibria within the low-temperature reaction pathways, such that, dissociation of $R\dot{O}_2$ and of $\dot{O}_2QOOH$ back to their respective radicals and O_2 have become more favorable. This is coupled with a shift in equilibrium between $R\dot{O}_2$ and $\dot{Q}OOH$ radicals favoring $R\dot{O}_2$ and also between these species and the products of their respective chain propagating pathways, favoring the products. These changes, in combination, have led to a decrease in the flux through the "alternative" reaction pathways, thus reducing their effect on the prediction of overall reactivity. With such a complex interplay between the major low-temperature reaction pathways and the sensitivity of model predictions to their relative contributions, it is crucial that the thermochemistry is accurate and consistent throughout and that thermochemical equilibrium is not restricted by definition of forward and reverse rate coefficients. Definition of rate coefficients in this manner completely circumvents the consideration of accurate thermochemistry. This defeats the purpose of thermochemistry by not allowing microscopic reversibility to hold and allows the use of wildly inaccurate rate coefficients which can still result in a model that can replicate overall reactivity.

An explanation to the discrepancies between rate coefficient assignments for *n*-heptane and *iso*-octane for the isomerization reactions of $R\dot{O}_2$ and of $\dot{O}_2QOOH$ has been proposed. We find that it is not suitable to treat the isomerization reactions of $\dot{O}_2QOOH$ to produce a carbonyl-hydroperoxide and a hydroxyl radical by analogy to the isomerization reactions of $R\dot{O}_2$ to produce a hydroperoxyl-alkyl radical. We find that rate coefficients from the literature are suitable for application to straight- and branched-chained alkanes.[17]

With major updates to thermochemical properties values and recommended rate rules, along with solutions to the long-standing discrepancies in the mechanisms of the PRFs, future work would entail applying the updated thermochemistry values, rate rules, and pathways used in this work to larger straight- and branched-chained alkanes. The oxidation of biofuels should also be reconsidered in light of our results.

AUTHOR INFORMATION

Corresponding Author

*E-mail: henry.curran@nuigalway.ie. Tel: +35391493856.

Notes

The authors declare no competing financial interest.

ACKNOWLEDGMENTS

The authors would like to acknowledge the support of the Irish Research Council in funding this work. We would also like to thank Drs. Sinéad Burke and Kuiwen Zhang at NUI Galway, Drs. Charlie Westbrook, Bill Pitz, and Marco Mehl at Lawrence Livermore National Laboratory, and Prof. Mani Sarathy at King Abdullah University of Science and Technology for helpful discussions and input.

REFERENCES

(1) Benson, S. W. *Thermochemical Kinetics*, 2nd ed.; Wiley: New York, 1976.

(2) Curran, H. J.; Gaffuri, P.; Pitz, W. J.; Westbrook, C. K. A Comprehensive Modeling Study of *n*-Heptane Oxidation. *Combust. Flame* **1998**, *114*, 149−177.

(3) Curran, H. J.; Gaffuri, P.; Pitz, W. J.; Westbrook, C. K. A Comprehensive Modeling Study of *iso*-Octane Oxidation. *Combust. Flame* **2002**, *129*, 253−280.

(4) Knox, J. H. In *Photochemistry and Reaction Kinetics*, Ashmore, P. G., Sugden, T. M., Dainton, F. S., Eds.; Cambridge University Press: Cambridge, 1967.

(5) Fish, A. *In Oxidation of Organic Compounds−II*, Mayo, F. R., Ed.; Advances in Chemistry Series 76; American Chemical Society: Washington, D. C., 1968; Vol. 2, p 69.

(6) Pollard, R. T. In *Comprehensive Chemical Kinetics: Gas-Phase Combustion*, Bamford, C. H., Tipper, C. F. H., Eds.; Elsevier: Amsterdam, 1977; Vol. *17*.

(7) Cox, R. A.; Cole, J. A. Chemical Aspects of the Autoignition of Hydrocarbon/air Mixtures. *Combust. Flame* **1985**, *60*, 109−123.

(8) Walker, R. W.; Morley, C. In *Comprehensive Chemical Kinetics: Low-Temperature Combustion and Autoignition*, Pilling, M. J., Ed.; Elsevier: Amsterdam, 1997; Vol. *35*.

(9) Silke, E. J. *Influence of Fuel Structure on Combustion as Demonstrated by the Isomers of Heptane: a Rapid Compression Machine Study & Detailed Kinetic Modelling of n-Heptane*. Ph.D. Thesis, School of Chemistry, NUI Galway, 2005.

(10) Glaude, P. A.; Battin-Leclerc, F.; Fournet, R.; Warth, V.; Côme, G. M.; Scacchi, G. Construction and Simplification of a Model for the Oxidation of Alkanes. *Combust. Flame* **2000**, *122*, 451−462.

(11) Ciezki, H. K.; Adomeit, G. Shock-tube Investigation of Self-Ignition of *n*-Heptane-Air Mixtures under Engine Relevant Conditions. *Combust. Flame* **1993**, *93*, 421−433.

(12) Villano, S. M.; Huynh, L. K.; Carstensen, H. H.; Dean, A. M. High-Pressure Rate Rules for Alkyl + O_2 Reactions. 1. The Dissociation, Concerted Elimination, and Isomerization Channels of the Alkyl Peroxy Radical. *J. Phys. Chem. A* **2011**, *115*, 13425−13442.

(13) Villano, S. M.; Huynh, L. K.; Carstensen, H. H.; Dean, A. M. High-Pressure Rate Rules for Alkyl + O_2 Reactions. 2. The

DOI: 10.1021/acs.jpca.5b00837
J. Phys. Chem. A 2015, 119, 7510−7527

Isomerization, Cyclic Ether Formation, and β-Scission Reactions of Hydroperoxy Alkyl Radicals. *J. Phys. Chem. A* **2012**, *116*, 5068−5089.
(14) Miyoshi, A. Molecular Size Dependent Falloff Rate Constants for the Recombination Reactions of Alkyl Radicals with O_2 and Implications for Simplified Kinetics of Alkylperoxy Radicals. *Int. J. Chem. Kin.* **2012**, *44*, 59−74.
(15) Goldsmith, C. F.; Green, W. H.; Klippenstein, S. J. Role of O_2 + QOOH in Low-Temperature Ignition of Propane. 1. Temperature and Pressure Dependent Rate Coefficients. *J. Phys. Chem. A* **2012**, *116*, 3325−3346.
(16) Miyoshi, A. Systematic Computational Study on the Unimolecular Reactions of Alkylperoxy (RO_2), Hydroperoxyalkyl (QOOH), and Hydroperoxyalkylperoxy (O_2QOOH) Radicals. *J. Phys. Chem. A* **2011**, *115*, 3301−3325.
(17) Sharma, S.; Raman, S.; Green, W. H. Intramolecular Hydrogen Migration in Alkylperoxy and Hydroperoxyalkylperoxy Radicals: Accurate Treatment of Hindered Rotors. *J. Phys. Chem. A* **2010**, *114*, 5689−5701.
(18) Brett, L. *Re-Commissioning of a Rapid Compression Machine and Computer Modelling of Hydrogen and Methane Autoignition*. Ph.D. Thesis, School of Chemistry, NUI Galway, 1999.
(19) Bugler, J.; Marks, B.; Mathieu, O.; Archuleta, R.; Heufer, K. A.; Petersen, E. L.; Curran, H. J. An Experimental and Modelling Study of Shock Tube and Rapid Compression Machine Ignition of the Pentane Isomers. 2015, to be submitted for publication.
(20) Healy, D.; Kalitan, D. M.; Aul, C. J.; Petersen, E. L.; Bourque, G.; Curran, H. J. Oxidation of C_1−C_5 Alkane Quinternary Natural Gas Mixtures at High Pressures. *Energy Fuels* **2010**, *24*, 1521−1528.
(21) Ribaucour, M.; Minetti, R.; Sochet, L. R.; Curran, H. J.; Pitz, W. J.; Westbrook, C. K. Ignition of Isomers of Pentane: An Experimental and Kinetic Modeling Study. *Proc. Combust. Inst.* **2000**, *28*, 1671−1678.
(22) Ritter, E. R.; Bozzelli, J. W. THERM: Thermodynamic Property Estimation for Gas Phase Radicals and Molecules. *Int. J. Chem. Kin.* **1991**, *23*, 767−778.
(23) Burke, S. M.; Simmie, J. M.; Curran, H. J. Critical Evaluation of Thermochemical Properties of C_1−C_4 Species: Updated Group-Contributions to Estimate Thermochemical Properties. *J. Phys. Chem. Ref. Data* **2015**, *44*, 013101.
(24) Kéromnès, A.; Metcalfe, W. K.; Heufer, K. A.; Donohoe, N.; Das, A. K.; Sung, C. J.; Herzler, J.; Naumann, C.; Griebel, P.; Mathieu, O.; et al. An Experimental and Detailed Chemical Kinetic Modeling Study of Hydrogen and Syngas Mixture Oxidation at Elevated Pressures. *Combust. Flame* **2013**, *160*, 995−1011.
(25) Metcalfe, W. K.; Burke, S. M.; Ahmed, S. S.; Curran, H. J. A Hierarchical and Comparative Kinetic Modeling Study of C_1−C_2 Hydrocarbon and Oxygenated Fuels. *Int. J. Chem. Kin.* **2013**, *45*, 638−675.
(26) Burke, S. M.; Metcalfe, W. K.; Herbinet, O.; Battin-Leclerc, F.; Haas, F. M.; Santner, J.; Dryer, F. L.; Curran, H. J. An Experimental and Modeling Study of Propene Oxidation. Part 1: Speciation Measurements in Jet-stirred and Flow Reactors. *Combust. Flame* **2014**, *161*, 2765−2784.
(27) Burke, U.; Somers, K. P.; O'Toole, P.; Zinner, C. M.; Marquet, N.; Bourque, G.; Petersen, E. L.; Metcalfe, W. K.; Serinyel, Z.; Curran, H. J. An Ignition Delay and Kinetic Modelling Study of Methane, Dimethyl ether, and Their Mixtures at High Pressures. *Combust. Flame* **2015**, *162*, 315−330.
(28) Karwat, D. M. A.; Wagnon, S. W.; Wooldridge, M. S.; Westbrook, C. K. Low-temperature Speciation and Chemical Kinetic Studies of *n*-Heptane. *Combust. Flame* **2013**, *160*, 2693−2706.
(29) Zádor, J.; Huang, H.; Welz, O.; Zetterberg, J.; Osborn, D. L.; Taatjes, C. A. Directly Measuring Reaction Kinetics of QOOH: A Crucial but Elusive Intermediate in Hydrocarbon Autoignition. *Phys. Chem. Chem. Phys.* **2013**, *15*, 10753−10760.
(30) Troe, J. The Thermal Dissociation/Recombination Reaction of Hydrogen Peroxide H_2O_2(+M) ↔ 2OH(+M) III.: Analysis and Representation of the Temperature and Pressure Dependence over Wide Ranges. *Combust. Flame* **2011**, *158*, 594−601.
(31) Ranzi, E.; Cavallotti, C.; Cuoci, A.; Frassoldati, A.; Pelucchi, M.; Faravelli, T. New Reaction Classes in the Kinetic Modeling of Low Temperature Oxidation of n-Alkanes. *Combust. Flame* **2015**, in press.
(32) Pelucchi, M.; Bissoli, M.; Cavallotti, C.; Cuoci, A.; Faravelli, T.; Frassoldati, A.; Ranzi, E.; Stagni, A. Improved Kinetic Model of the Low-Temperature Oxidation of *n*-Heptane. *Energy Fuels* **2014**, *28*, 7178−7193.
(33) Herbinet, O.; Husson, B.; Serinyel, Z.; Cord, M.; Warth, V.; Fournet, R.; Glaude, P. A.; Sirjean, B.; Battin-Leclerc, F.; Wang, Z.; et al. Experimental and Modeling Investigation of the Low-Temperature Oxidation of *n*-Heptane. *Combust. Flame* **2012**, *159*, 3455−3471.
(34) Battin-Leclerc, F.; Herbinet, O.; Glaude, P. A.; Fournet, R.; Zhou, Z.; Deng, L.; Guo, H.; Xie, M.; Qi, F. New Experimental Evidences about the Formation and Consumption of Ketohydroperoxides. *Proc. Combust. Inst.* **2011**, *33*, 325−331.
(35) Herbinet, O.; Battin-Leclerc, F.; Bax, S.; Le Gall, H.; Glaude, P. A.; Fournet, R.; Zhou, Z.; Deng, L.; Guo, H.; Xie, M.; Qi, F. Detailed Product Analysis During the Low Temperature Oxidation of n-Butane. *Phys. Chem. Chem. Phys.* **2011**, *13*, 296−308.
(36) Cord, M.; Husson, B.; Lizardo Huerta, J. C.; Herbinet, O.; Glaude, P. A.; Fournet, R.; Sirjean, B.; Battin-Leclerc, F.; Ruiz-Lopez, M.; Wang, Z.; et al. Study of the Low Temperature Oxidation of Propane. *J. Phys. Chem. A* **2012**, *116*, 12214−12228.
(37) Cord, M.; Sirjean, B.; Fournet, R.; Tomlin, A.; Ruiz-Lopez, M.; Battin-Leclerc, F. Improvement of the Modeling of the Low-Temperature Oxidation of *n*-Butane: Study of the Primary Reactions. *J. Phys. Chem. A* **2012**, *116*, 6142−6158.
(38) Bahrini, C.; Morajkar, P.; Schoemaecker, C.; Frottier, O.; Herbinet, O.; Glaude, P. A.; Battin-Leclerc, F.; Fittschen, C. Experimental and Modeling Study of the Oxidation of *n*-Butane in a Jet Stirred Reactor using cw-CRDS Measurements. *Phys. Chem. Chem. Phys.* **2013**, *15*, 19686−19698.
(39) Jalan, A.; Alecu, I. M.; Meana-Paneda, R.; Aguilera-Iparraguirre, J.; Yang, K. R.; Merchant, S. S.; Truhlar, D. G.; Green, W. H. New Pathways for Formation of Acids and Carbonyl Products in Low-Temperature Oxidation: The Korcek Decomposition of γ-Ketohydroperoxides. *J. Am. Chem. Soc.* **2013**, *135*, 11100−11114.
(40) Rolland, S.; Simmie, J. M. The Comparison of Detailed Chemical Kinetic Mechanisms; Forward Versus Reverse Rates with CHEMRev. *Int. J. Chem. Kin.* **2005**, *37*, 119−125.
(41) Jasper, A. W.; Miller, J. A. Lennard-Jones Parameters for Combustion and Chemical Kinetics Modeling from Full-Dimensional Intermolecular Potentials. *Combust. Flame* **2014**, *161*, 101−110.
(42) Pelucchi, M.; Somers, K. P.; Yasunaga, K.; Burke, U.; Frassoldati, A.; Ranzi, E.; Curran, H. J.; Faravelli, T. An Experimental and Kinetic Modeling Study of the Pyrolysis and Oxidation of *n*-C_3−C_5 Aldehydes in Shock Tubes. *Combust. Flame* **2015**, *162*, 265−286.
(43) Awan, I. A.; Burgess, D. R.; Manion, J. A. Pressure Dependence and Branching Ratios in the Decomposition of 1-Pentyl Radicals: Shock Tube Experiments and Master Equation Modeling. *J. Phys. Chem. A* **2012**, *116*, 2895−2910.
(44) Comandini, A.; Awan, I. A.; Manion, J. A. Thermal Decomposition of 1-Pentyl Radicals at High Pressures and Temperatures. *Chem. Phys. Lett.* **2012**, *552*, 20−26.
(45) Manion, J. A.; Awan, I. A. The Decomposition of 2-Pentyl and 3-Pentyl Radicals. *Proc. Combust. Inst.* **2013**, *34*, 537−545.
(46) Burke, M. P.; Goldsmith, C. F.; Georgievskii, Y.; Klippenstein, S. J. Towards a Quantitative Understanding of the Role of Non-Boltzmann Reactant Distributions in Low Temperature Oxidation. *Proc. Combust. Inst.* **2015**, *35*, 205−213.
(47) Goldsmith, C. F.; Burke, M. P.; Georgievskii, Y.; Klippenstein, S. J. Effect of Non-thermal Product Energy Distributions on Ketohydroperoxide Decomposition Kinetics. *Proc. Combust. Inst.* **2015**, *35*, 283−290.
(48) Cai, L.; Pitsch, H. Mechanism Optimization Based on Reaction Rate Rules. *Combust. Flame* **2014**, *161*, 405−415.

DOI: 10.1021/acs.jpca.5b00837
J. Phys. Chem. A 2015, 119, 7510−7527

(49) Huynh, L. K.; Carstensen, H. H.; Dean, A. M. Detailed Modeling of Low-Temperature Propane Oxidation: 1. The Role of the Propyl + O_2 Reaction. *J. Phys. Chem. A* **2010**, *114*, 6594−6607.
(50) Sheng, C. Y.; Bozzelli, J. W.; Dean, A. M.; Chang, A. Y. Detailed Kinetics and Thermochemistry of C_2H_5 + O_2: Reaction Kinetics of the Chemically-Activated and Stabilized CH_3CH_2OO Adduct. *J. Phys. Chem. A* **2002**, *106*, 7276−7293.
(51) Miller, J. A.; Klippenstein, S. J.; Robertson, S. H. A Theoretical Analysis of the Reaction Between Ethyl and Molecular Oxygen. *Proc. Combust. Inst.* **2000**, *28*, 1479−1486.
(52) Miller, J. A.; Klippenstein, S. J. The Reaction Between Ethyl and Molecular Oxygen II: Further Analysis. *Int. J. Chem. Kin.* **2001**, *33*, 654−668.
(53) DeSain, J. D.; Klippenstein, S. J.; Miller, J. A.; Taatjes, C. A. Measurements, Theory, and Modeling of OH Formation in Ethyl + O_2 and Propyl + O_2 Reactions. *J. Phys. Chem. A* **2003**, *107*, 4415−4427.
(54) Sun, H.; Bozzelli, J. W. Thermochemical and Kinetic Analysis on the Reactions of Neopentyl and Hydroperoxy-Neopentyl Radicals with Oxygen: Part I. OH and Initial Stable HC Product Formation. *J. Phys. Chem. A* **2004**, *108*, 1694−1711.
(55) *CHEMKIN-PRO 15101*; Reaction Design: San Diego, 2010.
(56) Mittal, G.; Raju, M. P.; Sung, C. J. CFD Modeling of Two-Stage Ignition in a Rapid Compression Machine: Assessment of Zero-Dimensional Approach. *Combust. Flame* **2010**, *157*, 1316−1324.
(57) Mittal, G.; Chomier, M. Effect of Crevice Mass Transfer in a Rapid Compression Machine. *Combust. Flame* **2014**, *161*, 398−404.
(58) Goldsborough, S. S.; Mittal, G.; Banyon, C. Methodology to Account for the Multi-stage Ignition Phenomena During Simulations of RCM Experiments. *Proc. Combust. Inst.* **2013**, *34*, 685−693.
(59) Mittal, G.; Bhari, A. A Rapid Compression Machine with Crevice Containment. *Combust. Flame* **2013**, *160*, 2975−2981.

DOI: 10.1021/acs.jpca.5b00837
J. Phys. Chem. A 2015, 119, 7510−7527